10.2 –
Global Dynamics of Engineering Systems

Giuseppe Rega

Department of Structural and Geotechnical Engineering
Sapienza University of Rome, Italy
Giuseppe.Rega@uniroma1.it

Coworkers: S. Lenci, P. Goncalves, M. Younis, D. Orlando, F. Silva, L. Ruzziconi, V. Settimi

DAY	TIME	LECTURE
Monday 05/11	14.00 -14.45	Historical Framework - A Global Dynamics Perspective in the Nonlinear Analysis of Systems/Structures
	15.00 -15.45	Achieving Load Carrying Capacity: Theoretical and Practical Stability
	16.00 -16.45	Dynamical Integrity: Concepts and Tools_1
Wednesday 07/11	14.00 -14.45	Dynamical Integrity: Concepts and Tools_2
	15.00 -15.45	**Global Dynamics of Engineering Systems**
	16.00 -16.45	Dynamical integrity: Interpreting/Predicting Experimental Response
Monday 12/11	14.00 -14.45	Techniques for Control of Chaos
	15.00 -15.45	A Unified Framework for Controlling Global Dynamics
	16.00 -16.45	Response of Uncontrolled/Controlled Systems in Macro- and Micro-mechanics
Wednesday 14/11	14.00 -14.45	A Noncontact AFM: (a) Nonlinear Dynamics and Feedback Control (b) Global Effects of a Locally-tailored Control
	15.00 -15.45	Exploiting Global Dynamics to Control AFM Robustness
	16.00 -16.45	Dynamical Integrity as a Novel Paradigm for Safe/Aware Design

Outline

1. **Global safety targets and related dynamical aspects**
   - **in operating conditions**
   - **towards extreme conditions**
2. **Using dynamic integrity**
3. **An overview of mechanical/structural systems addressed in the integrity perspective, from macro to nano**

Aspects of interest in a global safety perspective

Identifying global safety targets and related **dynamical aspects** (as regards variations of both i.c. and control parameters)

(i) in **operating conditions** → **competing attractors robustness**

verifying the relative robustness of coexisting bounded attractors of technical interest and the competition of their basins

(ii) towards **extreme conditions** → **basin erosion and system escape**

analyzing the erosion of the governing in-well safe basin encompassing different solutions, up to final escape of the response

Evaluating the safety

- selecting **proper integrity measures**

Improving the safety

- implementing **proper control techniques**

Operating conditions: attractor robustness (1)

Bistability: possibility to **jump to a coexisting bounded attractor**

- competition of resonant and non-resonant attractors in frequency- or force-response curves of single-dof oscillators

Undesirable, e.g., in AFM to improve imaging resolution:

- nearly identical vibration amplitudes at two different distances from sample can lead to hunting of feedback controller between them to maintain constant amplitude, which creates serious imaging artifacts

Desirable, e.g., in MEMS for activating a jump-driven hysteretic loop between competing responses:

- if used as **filters** $\longrightarrow$ interval with large oscillations bounded by ranges with small ones to be realized
- if used as **resonant sensors** $\longrightarrow$ lower (upper) oscillations expected before (after) detection of a physical parameter

Multistability: versatile system behavior valuable in some applications

Operating conditions: attractor robustness (2)

In global terms: the relative **size** of **competing basins**

safe jump from given attractor to a bounded coexisting one depends on topology of **basins**, which must be **adjacent to each other** (one generally surrounding the other)

Jump between pairs of a **variety/multiplicity of coexisting solutions**:

- with different periodicity competing with each other in same well
- in different wells (or in-well vs cross-well) of single-dof multi-well systems
- with different mechanical meaning competing with each other in multi-dof (and multi-well) systems

Analyzing **relative strength of competing attractor-basins** via **robustness profiles** through **different integrity measures**

Parametric pendulum: Oscillations vs Rotations

Competing attractors:

in-well vs **out-of-well**

(**oscillations**) (**rotations**)

both of interest for **harvesting energy** from **sea waves**

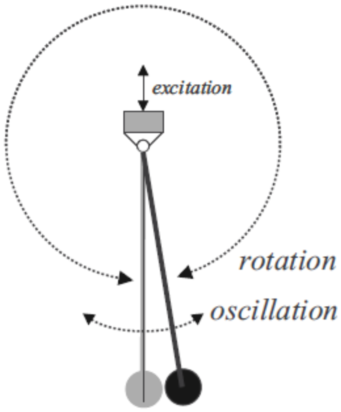

- **sharp** (oscillating) vs **flat** (rotating) IF profiles
- **optimal operating** conditions for **rotations**

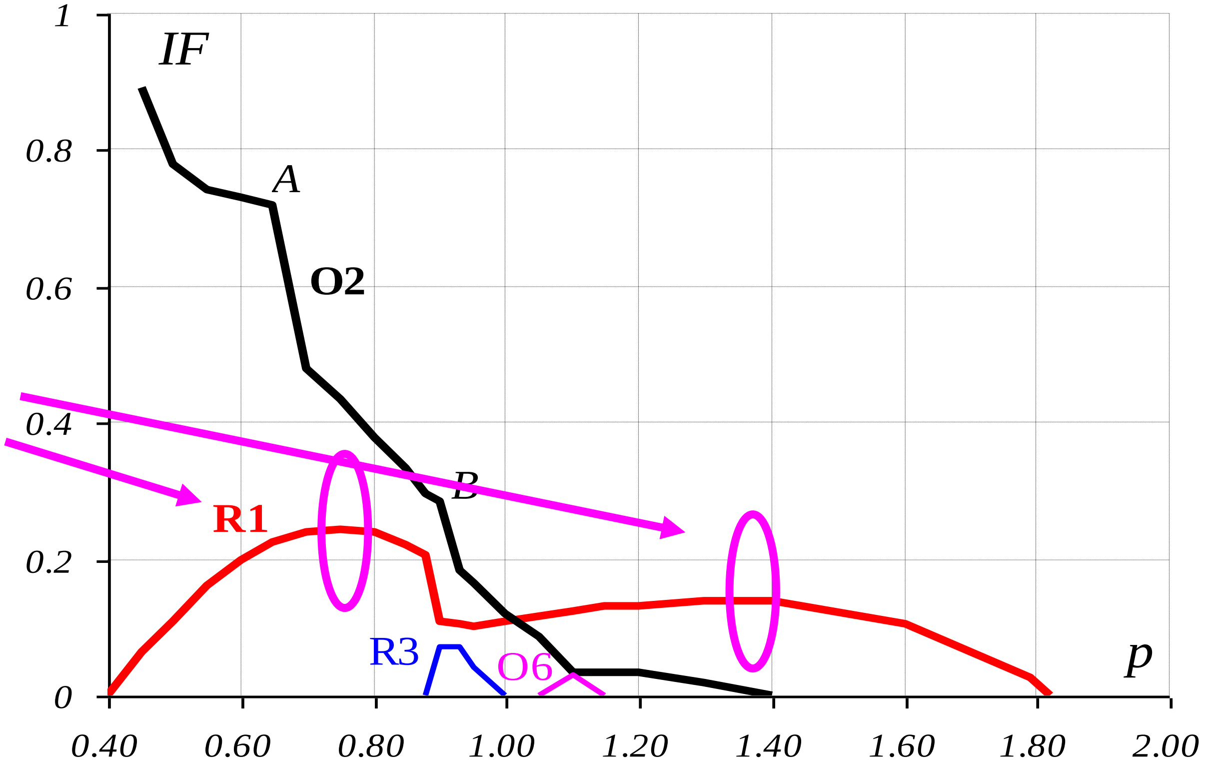

attractor robustness and basin integrity

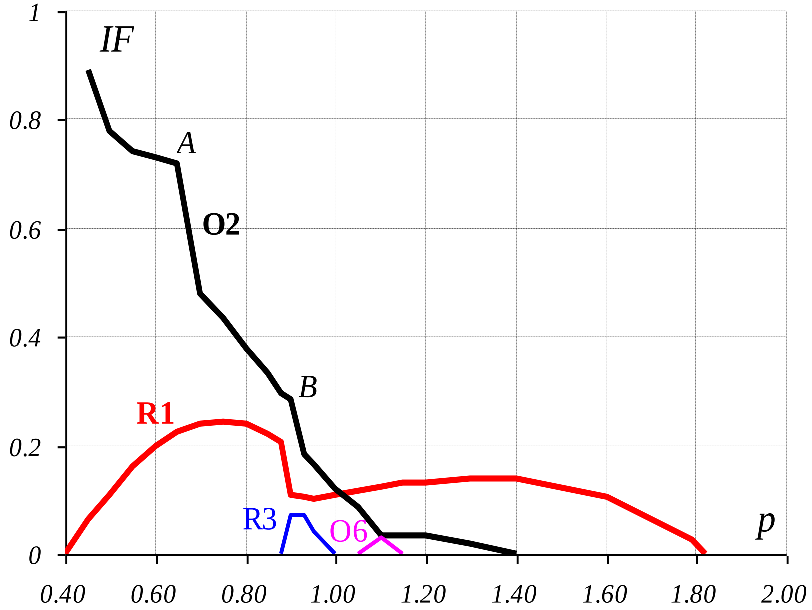

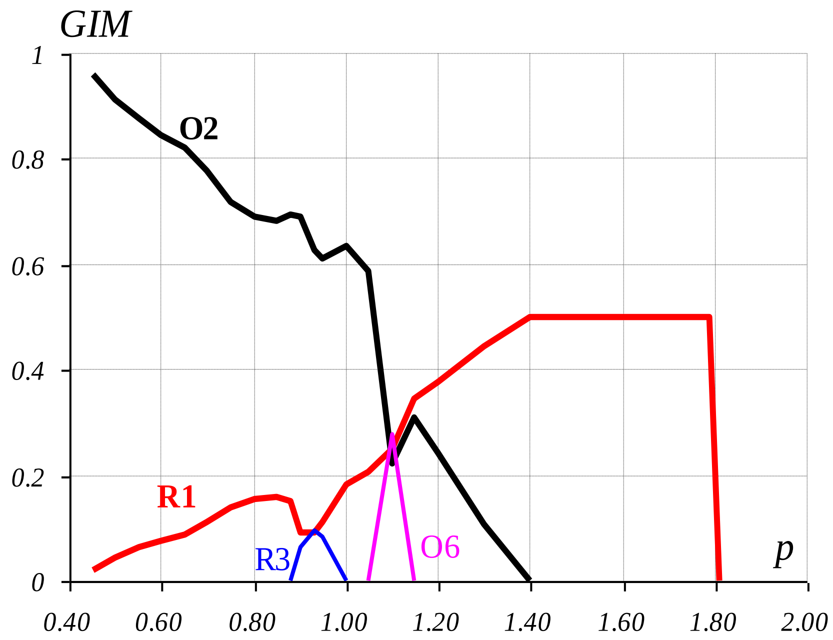

Comparing measures

e.g.: qualitative difference of IF and GIM:

- GIM: basically a measure of **attractor robustness**
- IF: also a measure of **basin integrity**, more interesting for **safe design**

Extreme conditions: system escape ……..

Systems with escape corresponding to ***different physical failures***:

ship ***capsizing***

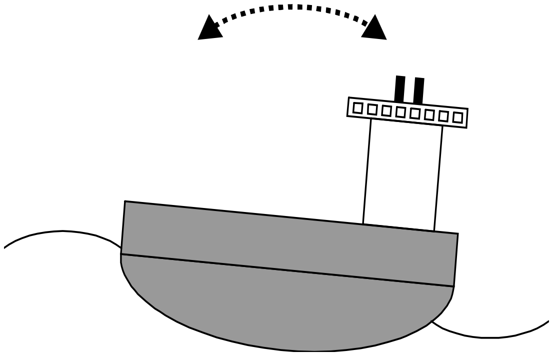

rigid block ***overturning***

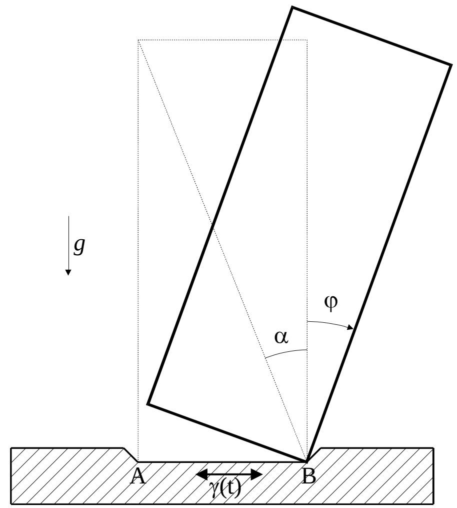

dynamic buckling of slender structures

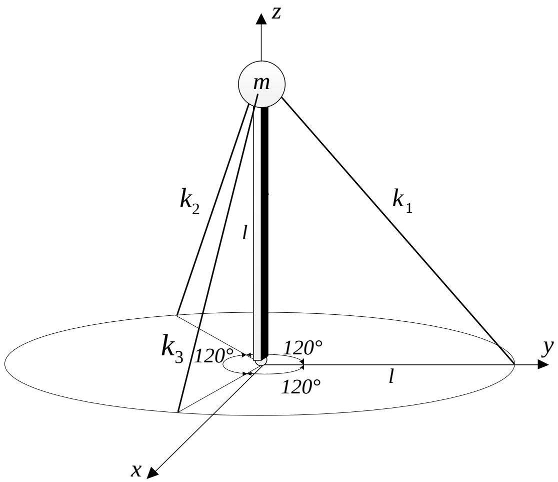

MEMS ***dynamic pull-in***

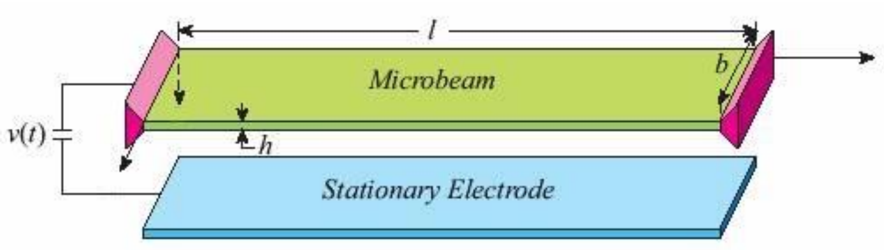

AFM ***jump-to-contact***

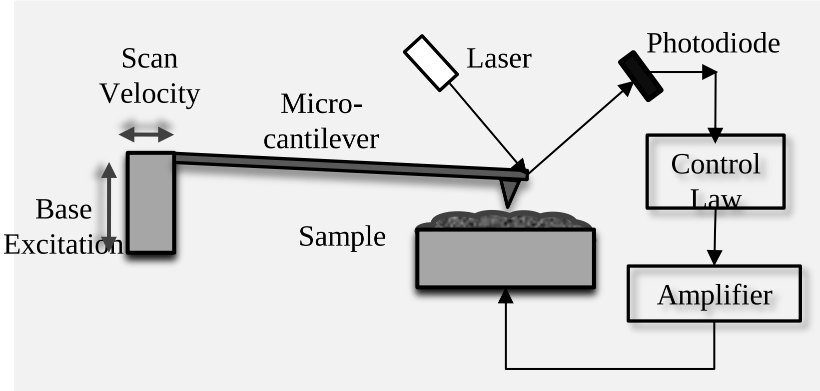

….. via basin erosion

Focus on

Overall safe basin of bounded responses, irrespective of which one is specifically realized

- **Basin size and compactness (integrity)** for *fixed* control parameters

- **Features of erosion** with a *varying* control parameter, which meaningfully affect the **rate of safety loss** before escape

Underlying **topological mechanisms** to be investigated in terms of governing saddles and associated invariant manifolds whose homoclinic or heteroclinic intersection triggers:

- the **start of erosion**

- its peculiar and possibly **dramatic features**

Models (mech-math), phase space, potential

an overall picture of dynamical problems

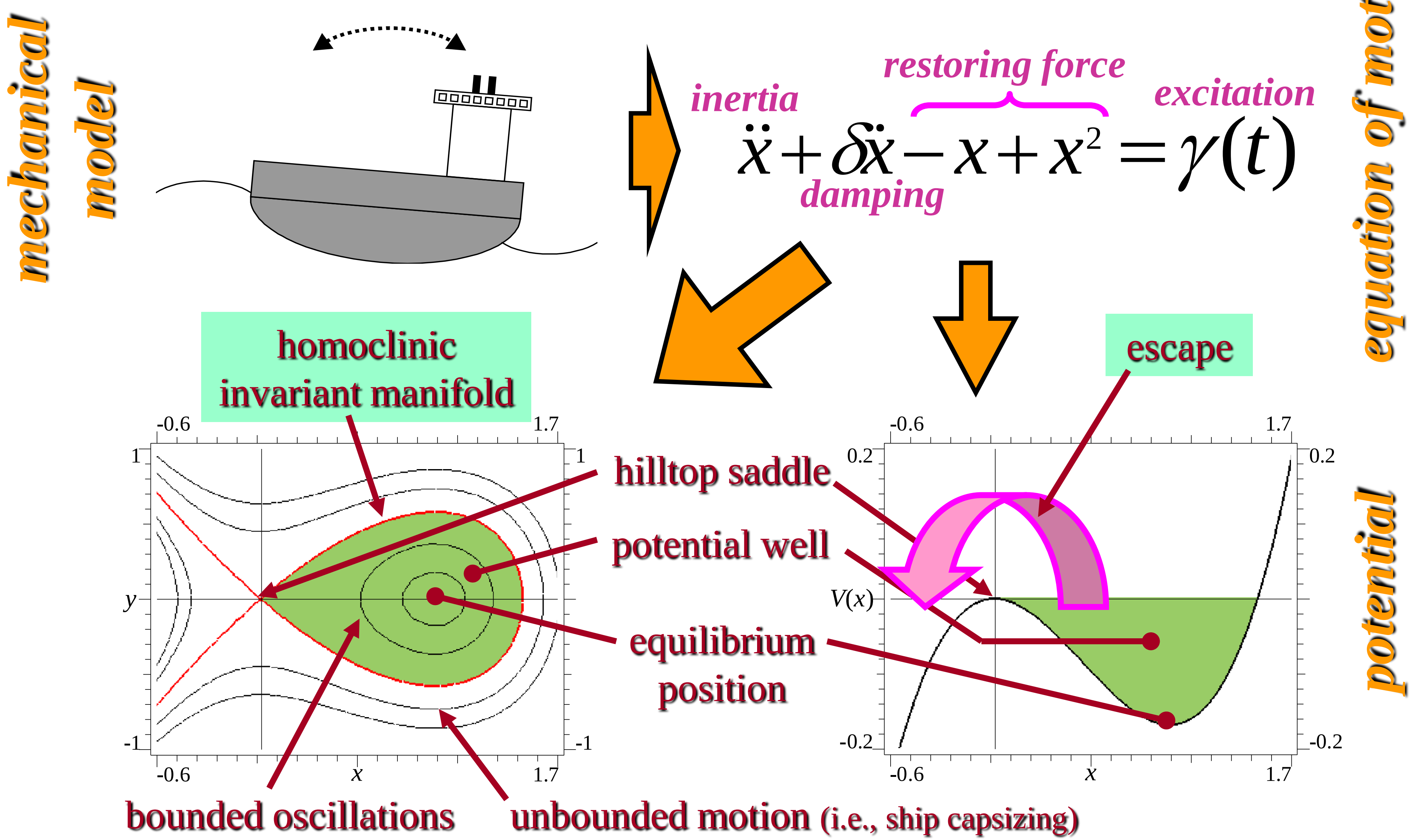

Erosion profiles

- integrity measures permit to study how the structure reliability changes when parameters vary
- **erosion profiles**: integrity measure as a function of **excitation amplitude**
- irrespective of safe basin definitions, exact/approximate information from:

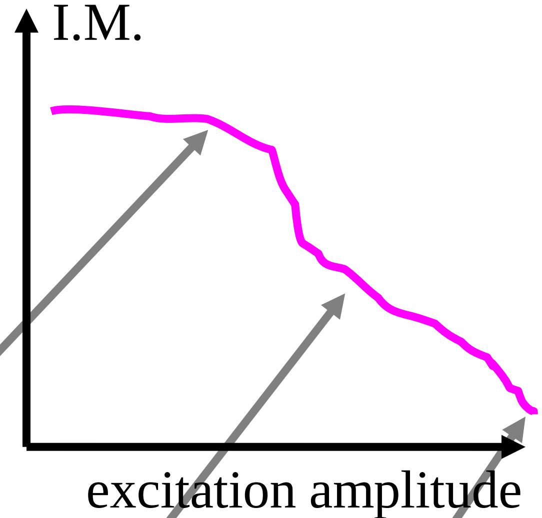

  - **homo/heteroclinic bifurcation** of the manifolds surrounding the potential well which triggers the erosion
  - then erosion proceeds with complex mechanisms, which may involve **secondary** homo/heteroclinic **bifurcations**
  - erosion ends with the onset of out-of-well phenomena which may represent the **physical “failure”**

Using dynamic integrity

Dynamic integrity referred to for

(i) **analyzing** global safety

(ii) **controlling** global safety

(iii) **interpreting** and **predicting** **experimental** behaviors through **theoretical models**

- **identifying unknown parameters**
- **detecting thresholds of applicability**

(iv) **formulating** **novel design criteria** which account for **robustness** and **erosion**, as well as **uncertainties**

Overall aims

Investigating dynamical integrity

of **different** nonlinear mechanical oscillators

- discussing specific **mechanical** issues
- discussing **dynamical** issues
- discussing **control** issues

different systems ⇨ different dynamical phenomena

Robustness/erosion profiles for

- **discrete** or **continuous** systems/models
- at **macro** or **micro/nano** scale

Mechanical and dynamical issues

Systems

- **Hardening** vs **softening**
- **Symmetric** vs **asymmetric**
- **Smooth** vs **non-smooth**
- **Resonant** vs **non-resonant**

Phenomena

- various “**failure**” : capsizing, overturning, pull-in, jump-to-contact, ……..
- different **integrity** measures
- **theory** vs **experiments**
- **uncontrol** vs **control** (of different, ***local*** or ***global***, nature)
- **harmonic** vs **stochastic** excitation

Mechanical/structural systems from macro to nano (1)

Archetypal oscillators: Duffing, Helmholtz, and combinations

Discrete systems in different configurations

- *von Mises truss*
- *Inverted impacting pendulum*
- Parametrically excited *pendulum*
- *Rigid block*
- *Inverted* (planar/spatial) *pendulums* with *asymmetric* or *symmetric* constraints
- Simplified model of a *guyed cantilever tower*
- Lumped model of a *capacitive accelerometer*
- *Primary linear* system with *nonlinear Tuned Mass Damper*

Mechanical/structural systems from macro to nano (2)

Reduced order models of **continuous systems**

- Single/two-mode models of *clamped microbeams*
- Single-mode model of a *carbon nanotube*
- Single-mode model of a noncontact *atomic force microcantilever*
- Single-mode model of a *suspension bridge*
- Single-mode model of a *cable-supported beam*
- Two-mode model of a post-buckled *cylindrical shell*

Mechanical/structural systems from macro to nano (3)

An overview from literature summarizing:

- Nonlinear **oscillator** and/or **mechanical system/model** in the background
- **Modeling**
  - **Discrete** systems: ODE of motion
  - **Continuous** systems: PDE (or integro-PDE) of motion

    Reduced order model (ROM)
- **Hamiltonian** system
  - Main **dynamical/mechanical** features: potential and/or phase portrait
- Excitation characteristics

Hardening: Duffing oscillator

Archetype of **hardening** **two-well symmetric** oscillators

Single-mode nonlinear dynamics of ***buckled beams, magnetoelastic pendulum***, and many others mechanical systems and structures

In-well vs Cross-well (***escape***) dynamics
Two equal, right and left, **homoclinic** orbits

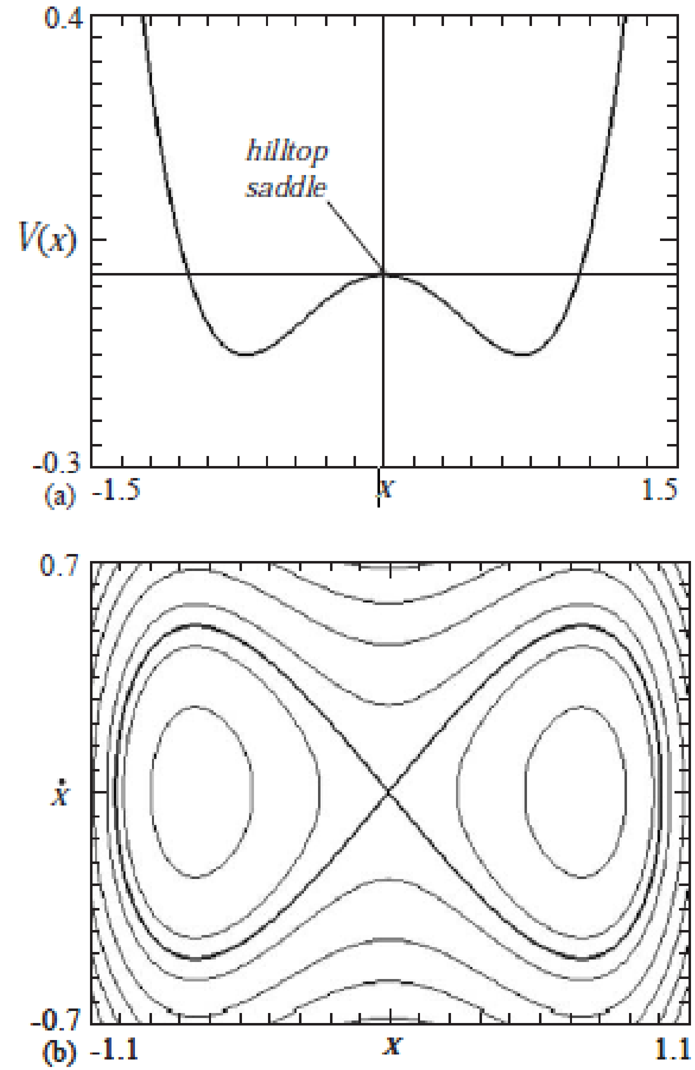

$$\ddot{x}+\varepsilon\delta\dot{x}-\frac{x}{2}+\frac{x^3}{2}=\varepsilon\gamma(\omega t)=\varepsilon\gamma_1\sum_{j=1}^{\infty}\frac{\gamma_j}{\gamma_1}\sin(j\omega t+\Psi$$

$\varepsilon\gamma_1$= overall excitation amplitude

γ_j/γ_1; Ψ_j= parameters governing the shape of the excitation

(Lenci and Rega, 2004a)

Hardening: Helmholtz-Duffing oscillator

Archetype of hardening two-well **asymmetric** oscillators

Single-mode nonlinear dynamics of one dimensional structural ***systems with initial curvature*** (shallow arches, buckled or imperfect beams)

In-well vs Cross-well (*escape*) dynamics

Two distinct, right and left, **homoclinic** orbits

$$\ddot{x} + \varepsilon\delta\dot{x} - \sigma x - \frac{3}{2}(\sigma - 1)x^2 + 2x^3 = \gamma_1 \sum_{j=1}^{\infty} \frac{\gamma_j}{\gamma_1} \sin(js + \Psi_j)$$

σ = measure of asymmetry

$\varepsilon\gamma_1$= overall excitation amplitude

γ_j/γ_1; Ψ_j= parameters governing the shape of the excitation

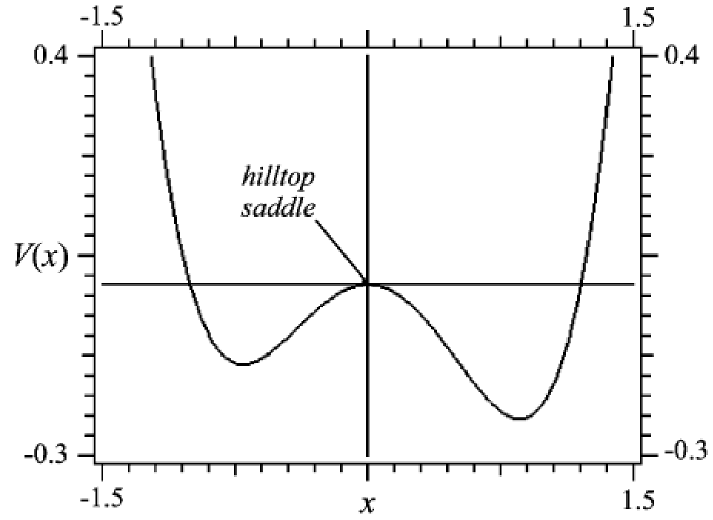

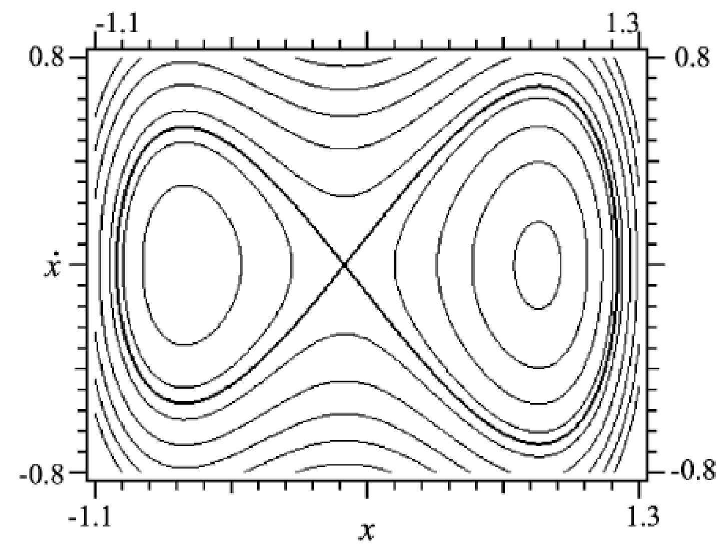

(Lenci and Rega, 2004a)

Shallow von-Mises truss

Planar version of shallow space trusses of pyramidal shape (geodesic domes, folding structures, carbon nanostructures)

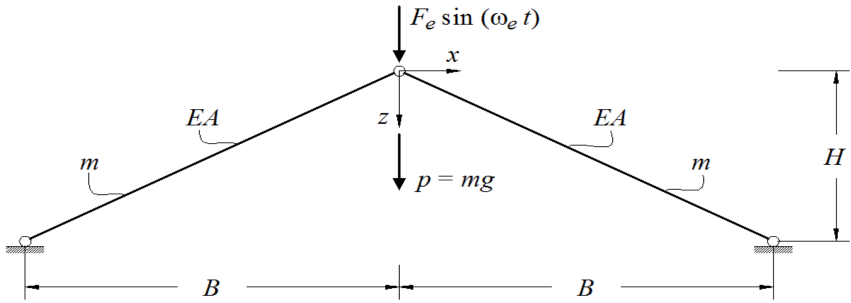

Prototype of **structural systems that may fail well below the theoretical limit point**

$$w_{,\tau\tau} + 2\xi w_{,\tau} + w\left(1 - 3w_i + 3/2\, w_i^2\right) - 3/2\, w^2\left(1 - w_i\right) + 1/2\, w^3 =$$
$$F\left(\sin(\Omega\tau) + \sum_{j=2}^{n} F_j/F \sin\left(j\Omega\tau + \upsilon_j\right)\right)$$

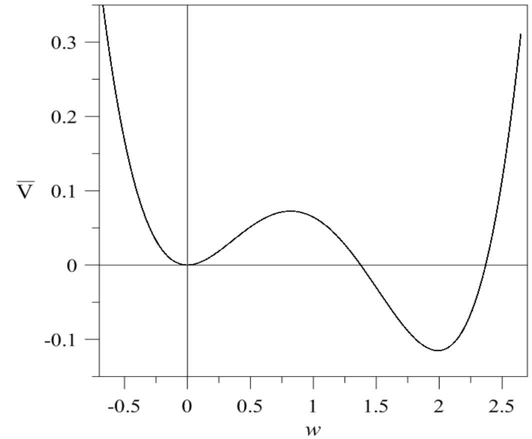

Compressive stresses lead to **unstable bifurcation along the nonlinear equilibrium path**

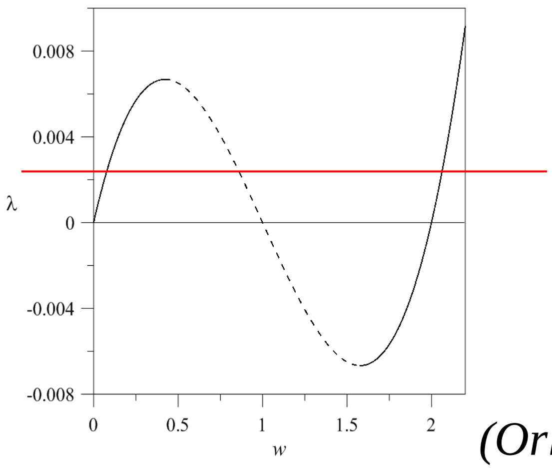

static load level equal to 30% of snap-through load

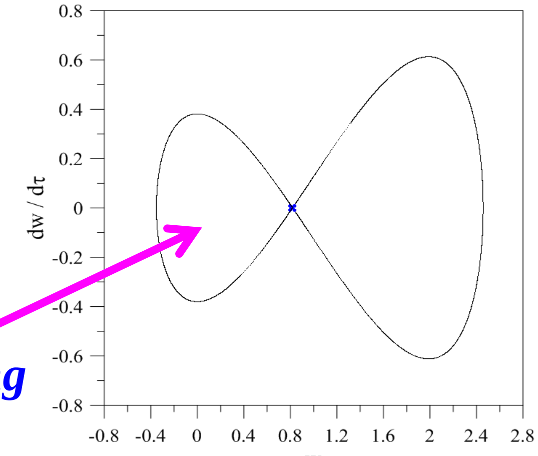

safe pre-buckling potential well

(Orlando et al, 2015)

Inverted impacting pendulum

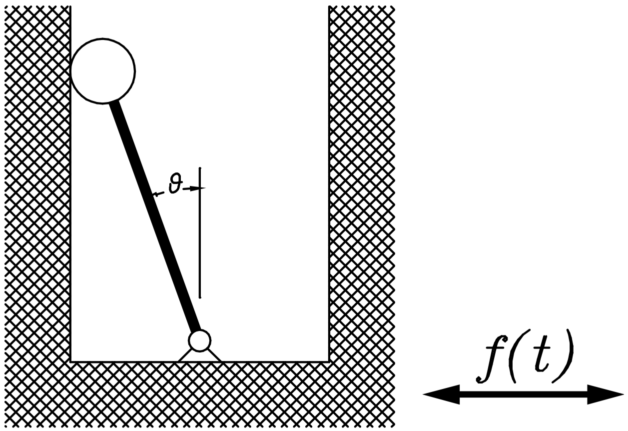

Equation of motion

$$\ddot{x}+\delta\dot{x}-x=\gamma_1\sum_{j=1}^{\infty}\frac{\gamma_j}{\gamma_1}\sin(j\omega t+\Psi_j),\qquad |x|<1$$

$$\dot{x}(t^+)=-r\dot{x}(t^-),\qquad |x|=1$$

generic periodic excitation

r = coefficient of restitution of unilateral constraints

Phase portrait

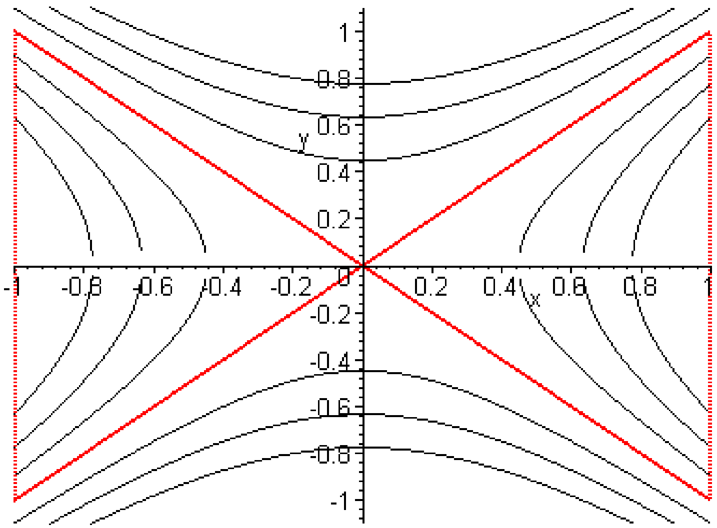

A **two-well** **impact** system with symmetric **homoclinic** orbits of the trivial saddle

(Lenci and Rega, 1998)

Softening: Helmholtz oscillator

Archetype of **softening** **single-well** **asymmetric** oscillators (***one escape*** direction)

Dynamics of ***systems in mechanics*** (***rolling asymmetric ships*** due to wind effects or asymmetric cargo, asymmetric cranes. prestressed membranes***) and applied sciences*** (bubble break-up, nonlinear waves/ solitons)

In-well vs Unbounded (***escape***) dynamics

One homoclinic orbit

$$\ddot{x}+0.1\dot{x}-x+x^2=\gamma(\omega t)=\gamma_1\sum_{j=1}^{\infty}\frac{\gamma_j}{\gamma_1}\sin(j\omega t+\Psi_j$$

$\varepsilon\gamma_1$= overall excitation amplitude

γ_j/γ_1; Ψ_j= parameters governing the shape of the excitation

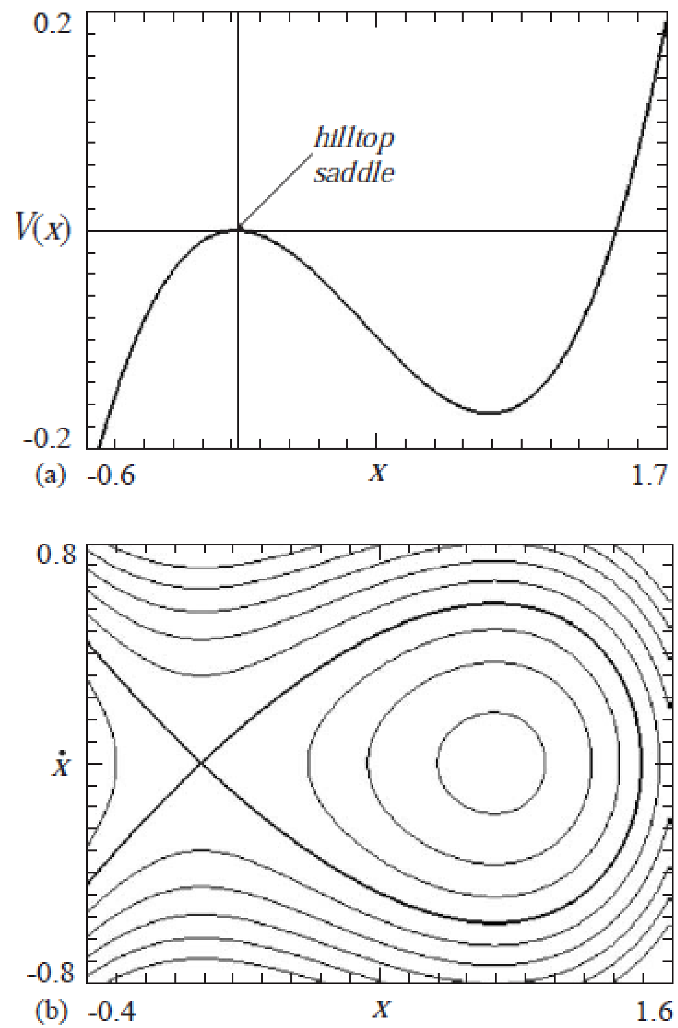

(Lenci and Rega, 2003)

Softening: Helmholtz-Duffing oscillator

Softening single-well asymmetric oscillator (***two unequal escape*** directions)

More realistic model of ***asymmetric ship rolling***, with a more accurate (third instead of second order) approximation of restoring hydrostatic potential

In-well vs (*two*) Unbounded (*escape*) dynamics
One homoclinic orbit of ***lower*** hilltop saddle

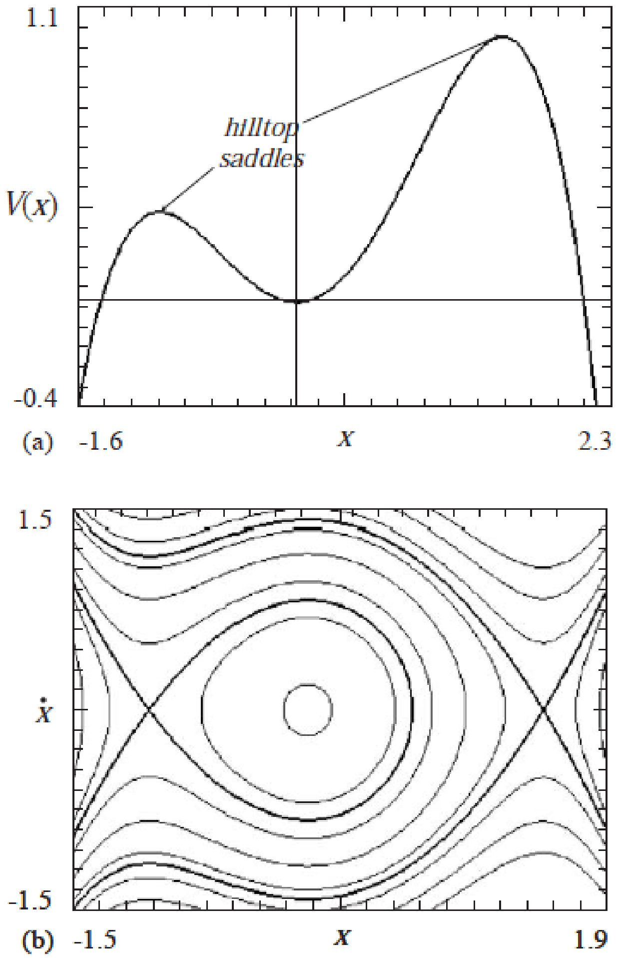

$$\ddot{x} + \varepsilon\delta\dot{x} + \sigma x + (\sigma - 1)x^2 - x^3 = \gamma_1 \sum_{j=1}^{\infty} \frac{\gamma_j}{\gamma_1} \sin(js + \Psi_j)$$

σ = measure of asymmetry ($\sigma = 1 \longrightarrow$ **Duffing single-well softening**: archetype for systems below subcritical pitchfork bifurcation; **two heteroclinic** orbits)

$\varepsilon\gamma_1$= overall excitation amplitude

γ_j/γ_1; Ψ_j= parameters governing the shape of the excitation

(Lenci and Rega, 2004b)

Parametrically excited mathematical pendulum

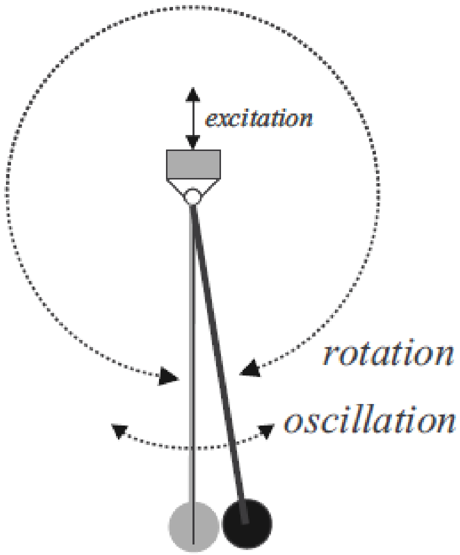

two homoclinic orbits of the coinciding hilltop saddle

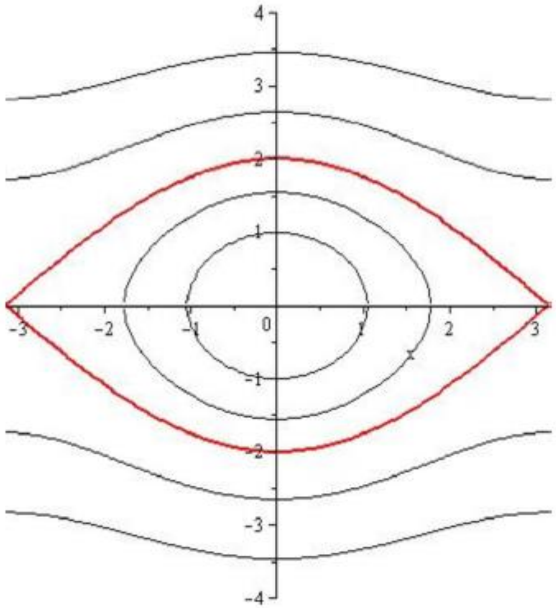

$$\ddot{x} + 0.1\dot{x} + [1 + p\cos(2t)]\sin(x) = 0$$

- in-well attractors (**oscillations**) versus out-of-well attractors (**rotations**)
- of interest for practical applications: **energy harvesting from rotations** excited by sea waves

(Lenci and Rega, 2008)

Rigid block

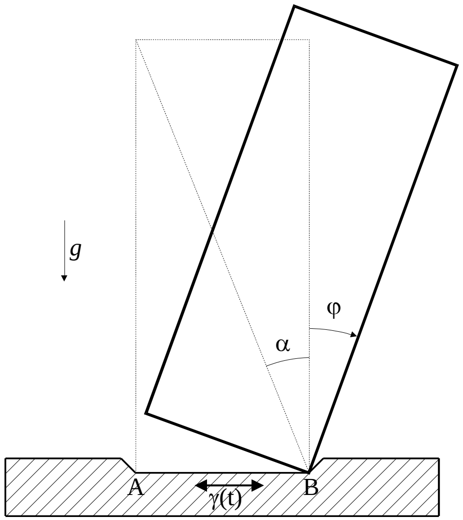

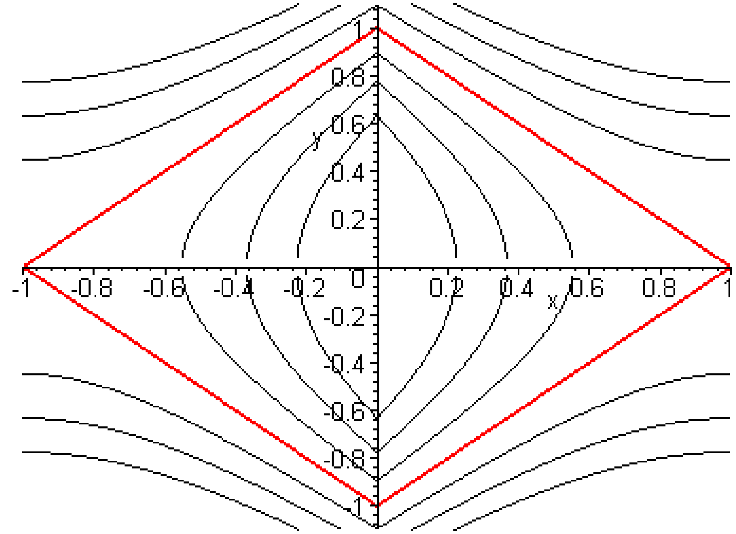

Two heteroclinic orbits

Rocking around the **left corner:**

$$\ddot{\varphi}+\delta\dot{\varphi}-\varphi-\alpha+\gamma(t)=0,\quad \varphi<0,$$

Rocking around the **right corner:**

$$\ddot{\varphi}+\delta\dot{\varphi}-\varphi+\alpha+\gamma(t)=0,\quad \varphi>0,$$

Impact (Newton law):

$$\dot{\varphi}(t^{+})=r\,\dot{\varphi}(t^{-}),\quad \varphi=0,$$

$T=2\pi/\omega$-periodic generic excitation:

$$\gamma(t)=\Sigma_j\,\gamma_j\cos(j\omega t+\psi_j)$$

Overturned positions φ=±π/2

(Lenci and Rega, 2005)

Augusti 2-dof model (4D)

perfect system

under horizontal
harmonic base excitation

geometrically
imperfect system

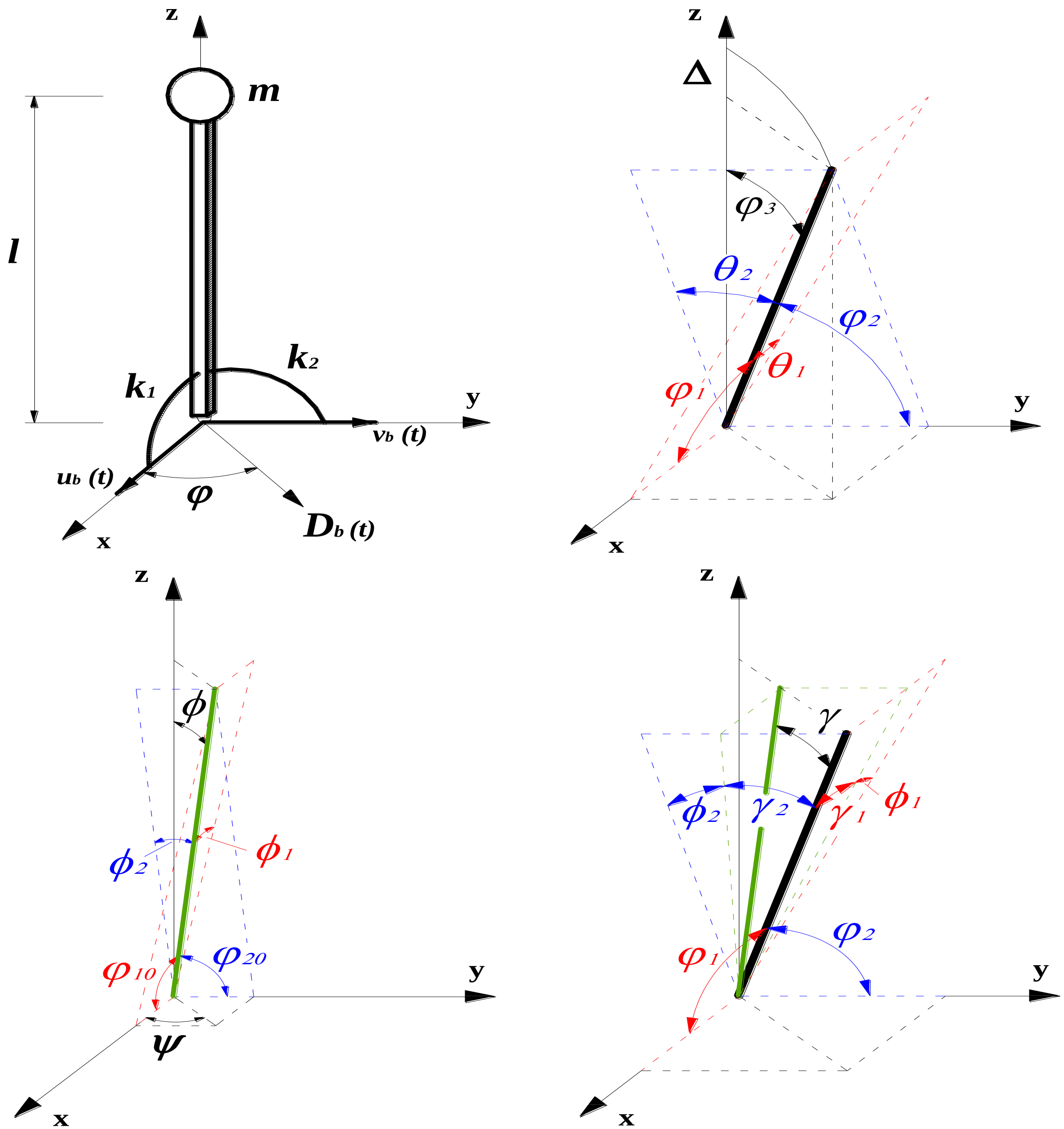

undeformed　　　　deformed

(Orlando et al, 2011)

Modeling

$$
\begin{aligned}
& ml^2\big(\ddot{\theta}_1(-\cos^2\theta_1\cos^2\theta_2+\cos^4\theta_1\cos^2\theta_2+\cos^2\theta_1\cos^4\theta_2) \\
& +\ddot{\theta}_2(-\cos\theta_1\sin\theta_1\cos\theta_2\sin\theta_2+\cos^3\theta_1\sin\theta_1\cos\theta_2\sin\theta_2 \\
& +\cos\theta_1\sin\theta_1\cos^3\theta_2\sin\theta_2)+\dot{\theta}_1^{\,2}(-\cos\theta_1\sin\theta_1\cos^4\theta_2 \\
& +\cos\theta_1\sin\theta_1\cos^2\theta_2)+\dot{\theta}_2^{\,2}(\cos\theta_1\sin\theta_1-2\cos\theta_1\sin\theta_1\cos^2\theta_2 \\
& -\cos^3\theta_1\sin\theta_1+2\cos^3\theta_1\cos^2\theta_2\sin\theta_1+\cos\theta_1\cos^4\theta_2\sin\theta_1) \\
& +\dot{\theta}_1\dot{\theta}_2(2\cos^2\theta_1\cos\theta_2\sin\theta_2-2\cos^4\theta_1\cos\theta_2\sin\theta_2)\big) \\
& +\left(C_1\dot{\theta}_1+k_1(\theta_1-\phi_1)-Pl\frac{\cos\theta_1\sin\theta_1}{\sqrt{1-\sin^2\theta_1-\sin^2\theta_2}}\right)(1-2\cos^2\theta_1 \\
& -2\cos^2\theta_2+\cos^4\theta_1+\cos^4\theta_2+2\cos^2\theta_1\cos^2\theta_2)=-ml\ddot{u}_b\cos\theta_1(1 \\
& -2\cos^2\theta_1-2\cos^2\theta_2+\cos^4\theta_1+\cos^4\theta_2+2\cos^2\theta_1\cos^2\theta_2)
\end{aligned}
$$

$$
\begin{aligned}
& ml^2\big(\ddot{\theta}_2(-\cos^2\theta_1\cos^2\theta_2+\cos^4\theta_1\cos^2\theta_2+\cos^2\theta_1\cos^4\theta_2) \\
& +\ddot{\theta}_1(-\cos\theta_1\sin\theta_1\cos\theta_2\sin\theta_2+\cos^3\theta_1\sin\theta_1\cos\theta_2\sin\theta_2 \\
& +\cos\theta_1\sin\theta_1\cos^3\theta_2\sin\theta_2)+\dot{\theta}_2^{\,2}(-\cos^4\theta_1\cos\theta_2\sin\theta_2 \\
& +\cos^2\theta_1\cos\theta_2\sin\theta_2)+\dot{\theta}_1^{\,2}(\cos\theta_2\sin\theta_2-2\cos^2\theta_1\cos\theta_2\sin\theta_2 \\
& -\cos^3\theta_2\sin\theta_2+2\cos^2\theta_1\cos^3\theta_2\sin\theta_2+\cos^4\theta_1\cos\theta_2\sin\theta_2) \\
& +\dot{\theta}_1\dot{\theta}_2(2\cos\theta_1\sin\theta_1\cos^2\theta_2-2\cos\theta_1\sin\theta_1\cos^4\theta_2)\big) \\
& +\left(C_2\dot{\theta}_2+k_2(\theta_2-\phi_2)-Pl\frac{\cos\theta_2\sin\theta_2}{\sqrt{1-\sin^2\theta_1-\sin^2\theta_2}}\right)(1-2\cos^2\theta_1 \\
& -2\cos^2\theta_2+\cos^4\theta_1+\cos^4\theta_2+2\cos^2\theta_1\cos^2\theta_2)=-ml\ddot{v}_b\cos\theta_2(1 \\
& -2\cos^2\theta_1-2\cos^2\theta_2+\cos^4\theta_1+\cos^4\theta_2+2\cos^2\theta_1\cos^2\theta_2)
\end{aligned}
$$

Coupled system: 2-dof (θ_1, θ_2)

$$
ml^2\left(\frac{\ddot{u}\left(-\cos^2\left(\frac{\sqrt{2}}{2}u\right)+2\cos^4\left(\frac{\sqrt{2}}{2}u\right)\right)+\frac{\sqrt{2}}{2}\dot{u}^2\cos\left(\frac{\sqrt{2}}{2}u\right)\sin\left(\frac{\sqrt{2}}{2}u\right)}{1-4\cos^2\left(\frac{\sqrt{2}}{2}u\right)+4\cos^4\left(\frac{\sqrt{2}}{2}u\right)}\right)
$$

$$
+C\dot{u}+k(u-\phi)-Pl\sqrt{2}\,\frac{\cos\left(\frac{\sqrt{2}}{2}u\right)\sin\left(\frac{\sqrt{2}}{2}u\right)}{\sqrt{1-2\sin^2\left(\frac{\sqrt{2}}{2}u\right)}}=-ml\frac{\sqrt{2}}{2}(\ddot{x}_b+\ddot{y}_b)\cos\left(\frac{\sqrt{2}}{2}u\right)
$$

Uncoupled system: 1-dof (u)

(excitation angle $\psi = 45°$)

Augusti model: 2-dof perfect

Perfect

(static load $\lambda = 0.9$)

Equilibrium paths

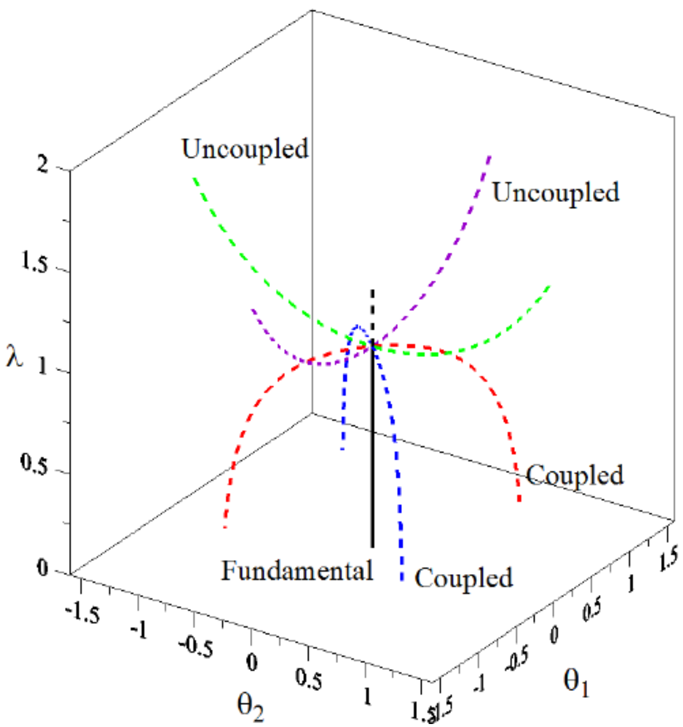

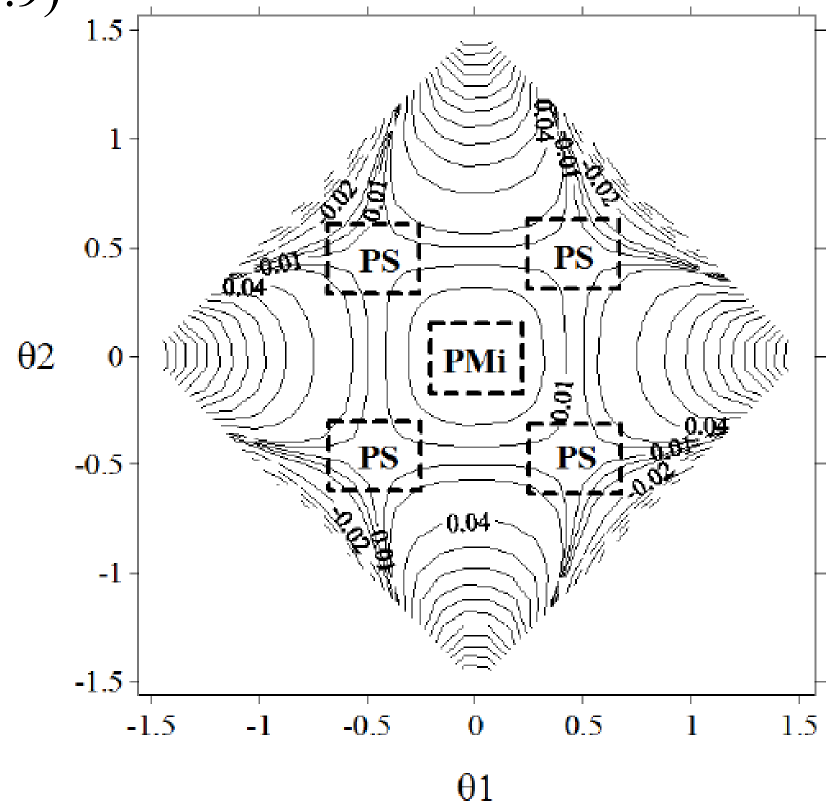

- four symmetric saddles $\longleftrightarrow$ four **unstable postbuckling** descending branches
- minimum point $\longleftrightarrow$ **stable prebuckling** solution

invariant manifolds of saddles separate i.c. leading to bounded solutions that surround the prebuckling configuration, and identify the **safe region**, from **unbounded escape** solutions

Augusti model: 2-dof imperfect

Imperfect

Equilibrium paths

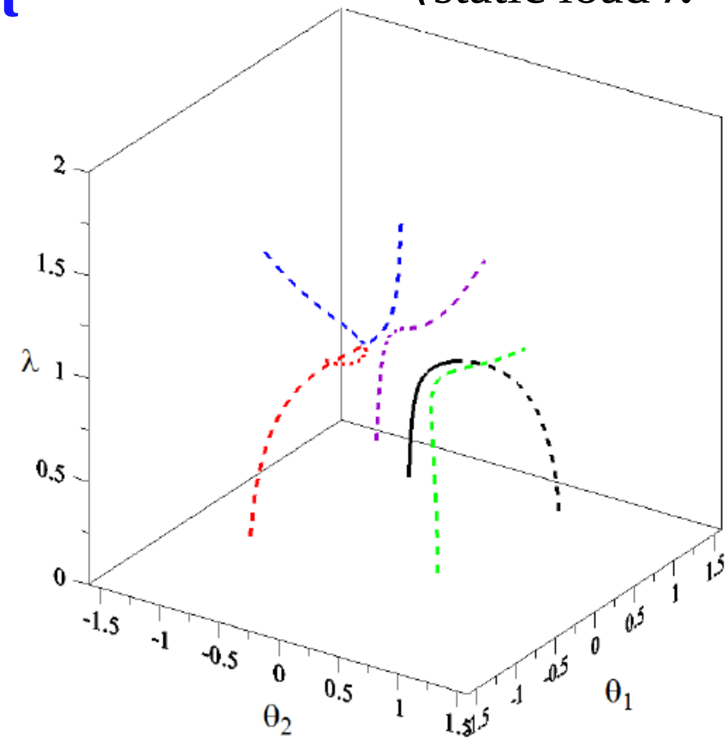

(static load λ = 0.9)

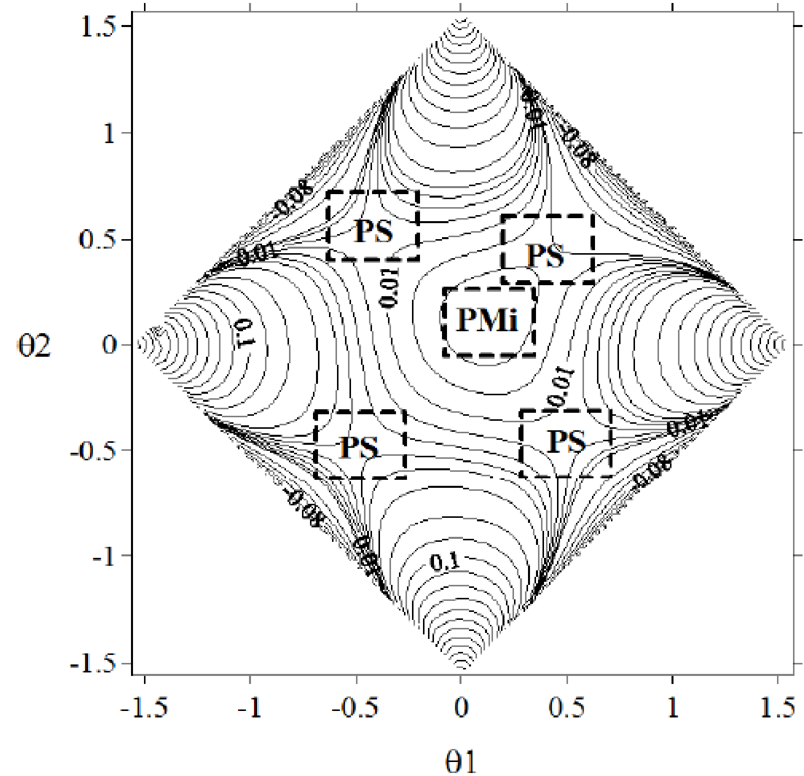

safe region bounded by the saddle, corresponding to the unstable black equilibrium path, with lowest potential energy among the four; it is much **smaller** than for **perfect** model

imperfections decrease both the **load-carrying capacity** of the structure and the **set of i.c.** that lead to **safe** bounded motions around equilibrium

Augusti model: 1-dof

Perfect

Two-dimensional projections in 4D

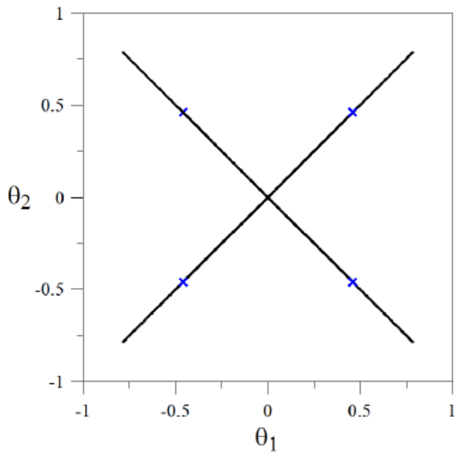

In 2D
(excitation angle $\psi = 45°$):

two heteroclinic orbits

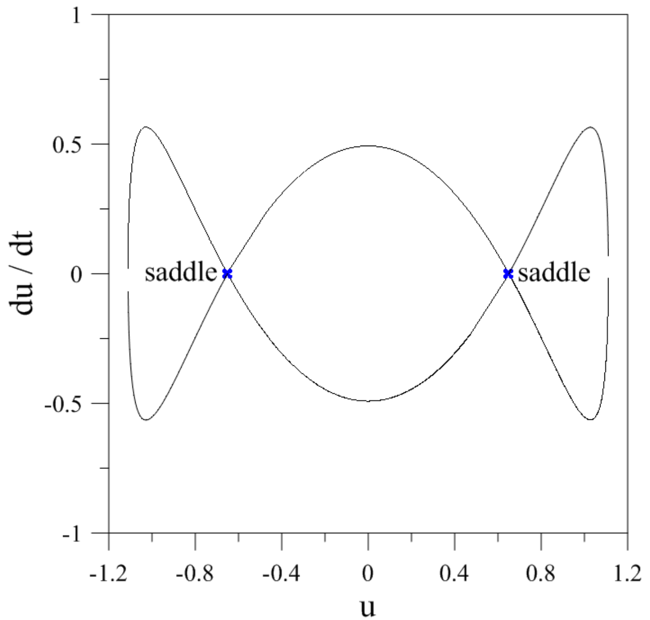

Imperfect

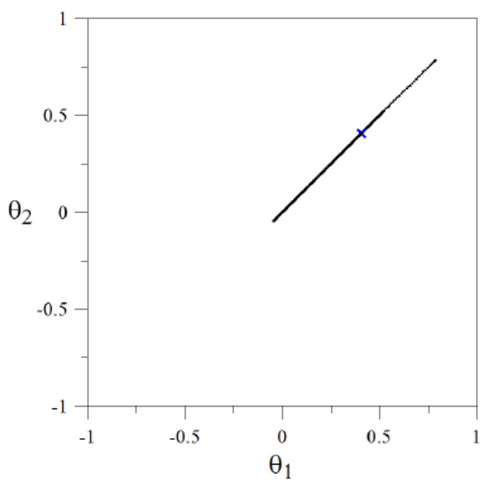

In 2D
(excitation angle $\psi = 45°$):

one homoclinic orbit

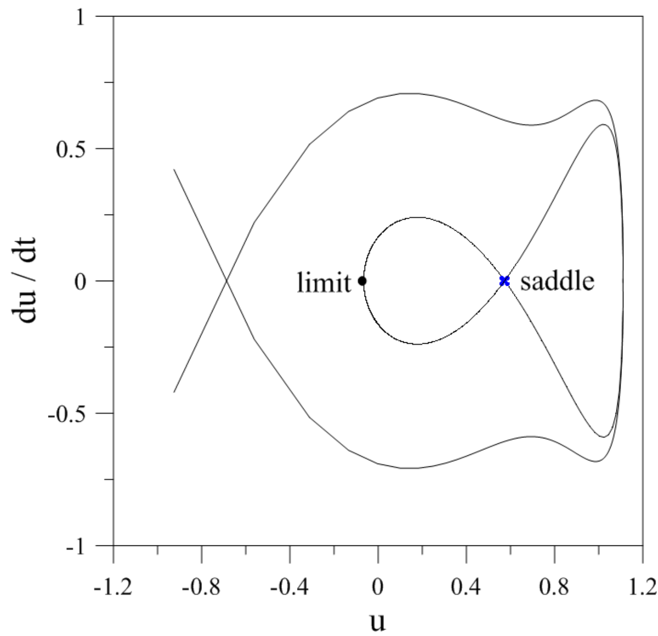

Guyed tower 2-dof model (4D)

Simplified model of a guyed tower stabilized by three equal linear springs, k_1, k_2 and k_3, inclined at 45° and located at 120° $\longrightarrow$ two coincident buckling loads

Horizontal harmonic base excitation $D_b(t)$

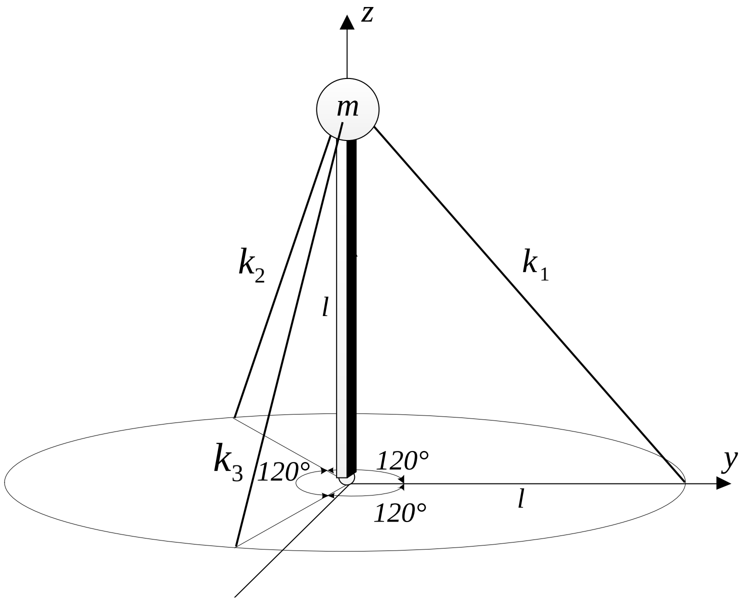

$$\ddot{u}_1(1-u_1^2-2u_2^2+u_1^2u_2^2+u_2^4)+\ddot{u}_2(u_1u_2-u_1^3u_2-u_1u_2^3)+\dot{u}_1^2(u_1-u_1u_2^2)+\dot{u}_2^2(u_1-u_1^3)+2u_1^2u_2\dot{u}_1\dot{u}_2+$$
$$\left[\frac{2}{\sqrt{3}\lambda\Omega^2}\left(\frac{\sqrt{2}}{\sqrt{2-\sqrt{3}u_1+u_2}}-\frac{\sqrt{2}}{\sqrt{2+\sqrt{3}u_1+u_2}}\right)-\frac{1}{\Omega^2}\frac{u_1}{\sqrt{1-u_1^2-u_2^2}}+\frac{2\xi_1}{\Omega}\dot{u}_1\right](-1+u_1^2+u_2^2)^2=$$
$$F\cos\varphi\sin\tau(-1+u_1^2+u_2^2)^2,$$

$$\ddot{u}_2(1-u_2^2-2u_1^2+u_1^2u_2^2+u_1^4)+\ddot{u}_1(u_1u_2-u_1^3u_2-u_1u_2^3)+\dot{u}_2^2(u_2-u_1^2u_2)+\dot{u}_1^2(u_2-u_2^3)+2u_1u_2^2\dot{u}_1\dot{u}_2+$$
$$\left[-\frac{2}{3\lambda\Omega^2}\left(\frac{\sqrt{2}}{\sqrt{2-\sqrt{3}u_1+u_2}}+\frac{\sqrt{2}}{\sqrt{2+\sqrt{3}u_1+u_2}}\right)+\frac{4}{3\lambda\Omega^2}\frac{\sqrt{2}}{\sqrt{2-2u_2}}-\right.$$
$$\left.\frac{1}{\Omega^2}\frac{u_2}{\sqrt{1-u_1^2-u_2^2}}+\frac{2\xi_2}{\Omega}\dot{u}_2\right](-1+u_1^2+u_2^2)^2=F\sin\varphi\sin\tau(-1+u_1^2+u_2^2)^2.$$

(Orlando et al, 2013)

Guyed tower: 1-dof

1-dof model if excited and with imperfection in one direction of symmetry

$$\frac{\ddot{u}(1-u^2)+u\dot{u}^2}{(-1+u^2)^2}+\frac{2\xi}{\Omega}\dot{u}+\frac{4}{3\lambda\Omega^2}\left(\frac{\sqrt{2-u_{10}}-\sqrt{2-u}}{\sqrt{2-u}}-\frac{\sqrt{2+2u_{10}}-\sqrt{2+2u}}{\sqrt{2+2u}}\right)-\frac{1}{\Omega^2}\frac{u}{\sqrt{1-u^2}}=F\sin(\tau)$$

Perfect

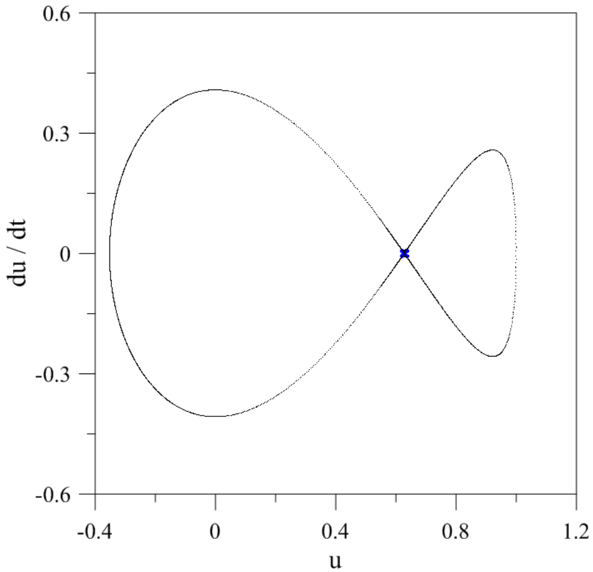

Imperfect

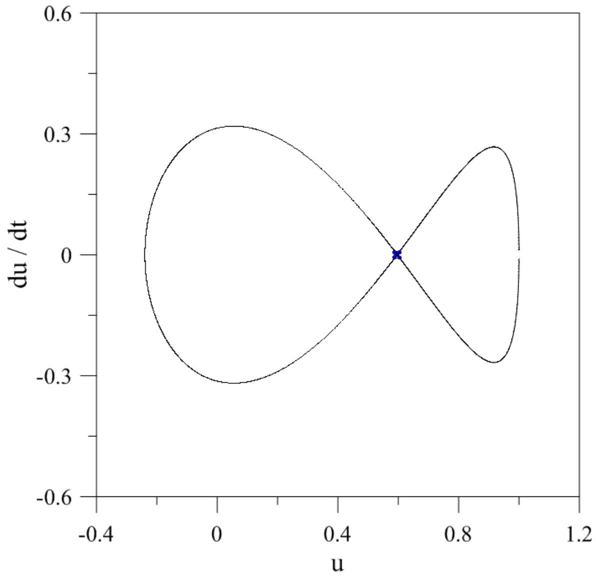

(static load $\lambda = 0.7$)

safe potential well always bounded by a **homoclinic orbit**

besides **lowering** the **stability threshold**, geometric **imperfection** somehow **reduces** the area, i.e. the **safety of equilibrium** for a given axial load

MEMS device: a capacitive accelerometer (1)

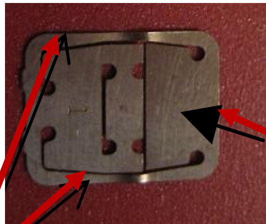

Upper electrode

proof mass
suspended by

two cantilever beams

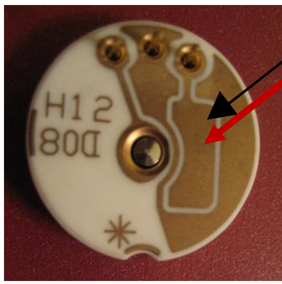

Lower electrode

placed underneath
the proof mass,
on a silicon substrate

Assembled sensor

(Alsaleem et al, 2010)

<u>Spring-mass single d.o.f model</u>

The device is modeled as a parallel plate ***capacitor*** with two rigid plates, where the upper one is ***movable***

- lumped mass → proof mass
- spring → two cantilever beams

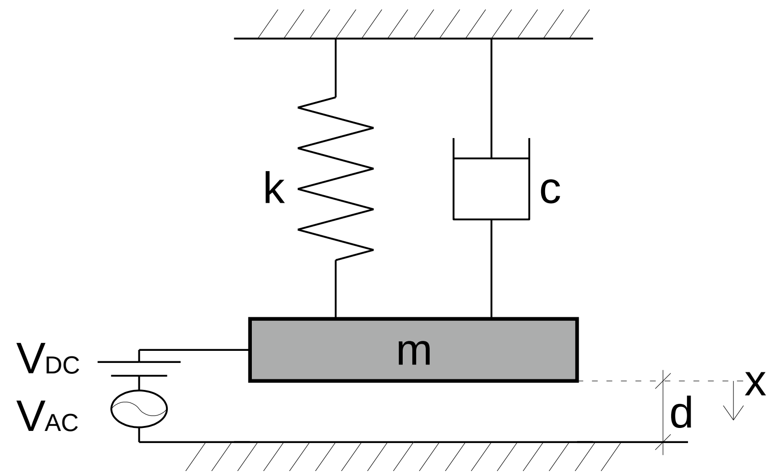

$$\boxed{m\ddot{x} + c\dot{x} + kx = \varepsilon A \frac{[V_{DC} + V_{AC}\cos(\Omega t)]^2}{2(d-x)^2}}$$

MEMS device: a capacitive accelerometer (2)

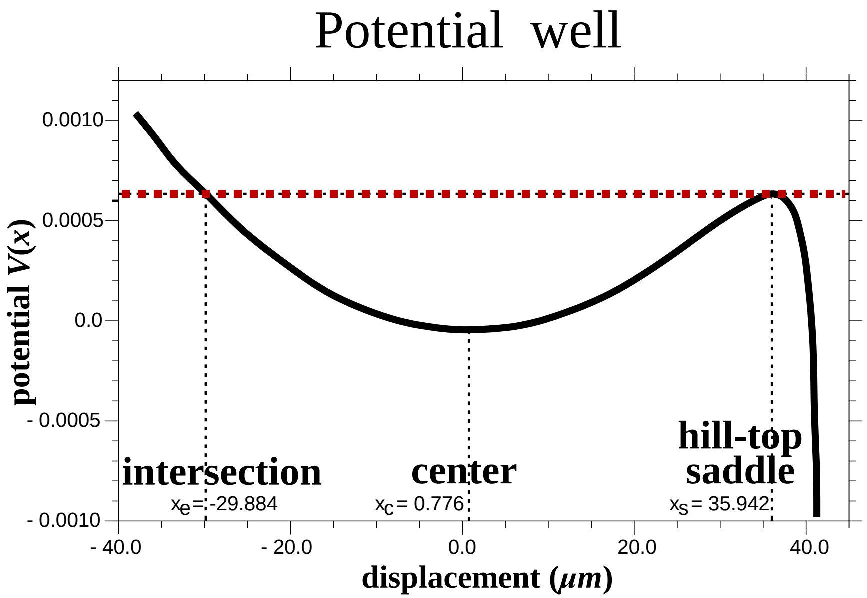

The unforced, undamped system is Hamiltonian with a **single asymmetric** potential well, of **softening** type, with **escape** direction

$$V(x) = k\frac{x^2}{2} - \frac{\varepsilon A V_{DC}^2}{2(d-x)}$$

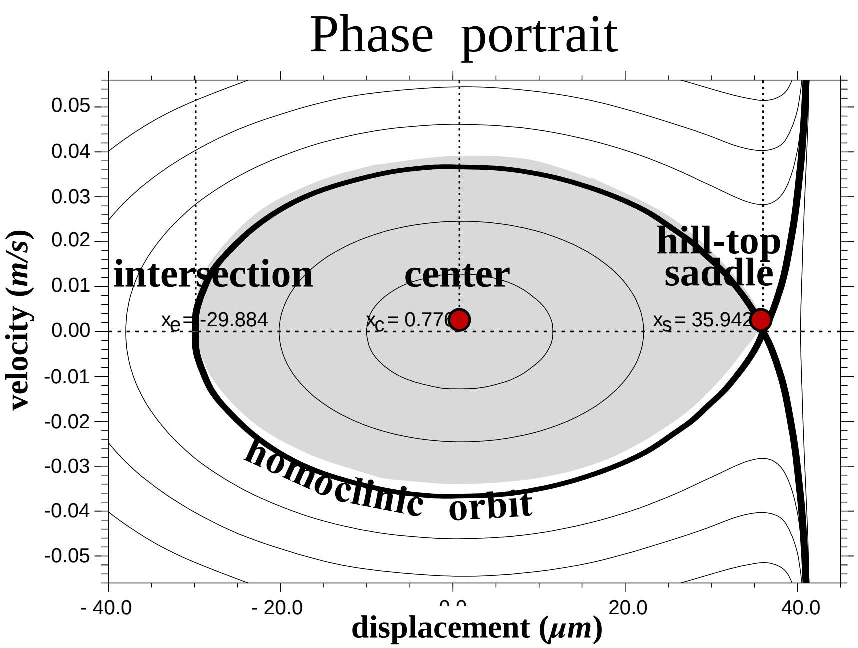

- Two equilibrium points: a *center* and a *hilltop saddle*
- Stable and unstable manifolds of the hilltop saddle coincide
- ***Homoclinic orbit*** separating in-well oscillations and out-of-well escape

MEMS: thermoelastic electrically actuated microbeam

(Gottlieb and Champneys, 2005)

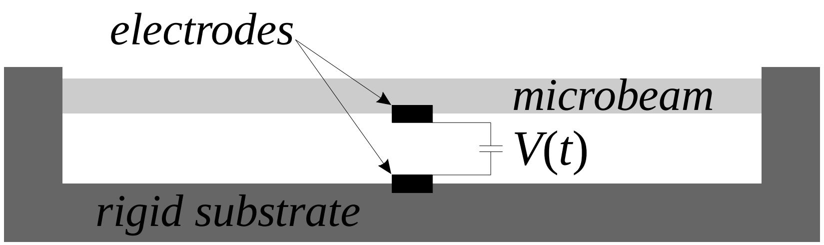

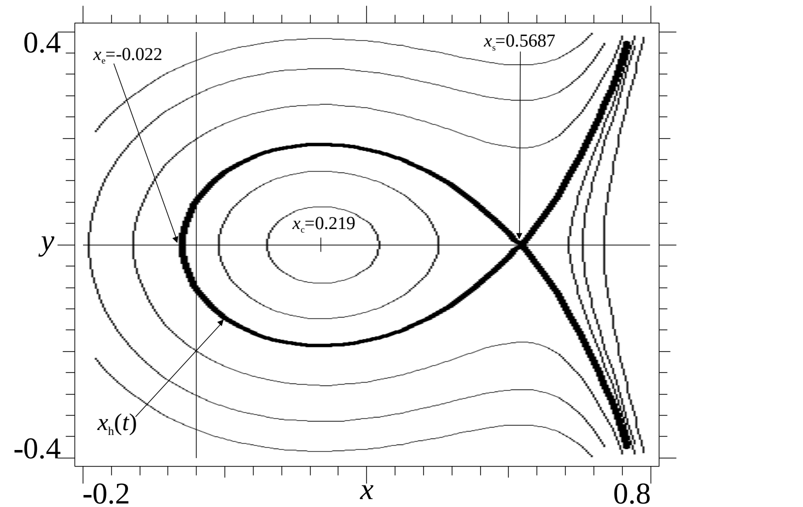

- small electrodynamic force
- small visco- and thermo-elastic damping

→ temperature condensation

Single-dof model

$$\ddot{x} + \alpha x + \beta x^3 - \frac{\gamma}{(1-x)^2} = \varepsilon\left\{ -\tilde{\mu}\dot{x} + \frac{\tilde{\eta}\sum_{j=1}^{N}(\eta_j/\eta_1)\sin(j\Omega t + \Psi_j)}{(1-x)^2} \right\}$$

substrate at x=1

overall excitation amplitude

$\gamma>0$	magnitude of electrostatic force, ≈ square of constant (DC) input voltage
Ω	frequency of periodic electrodynamic force
$\eta_j>0$ Ψ_j	relative amplitudes and phases of j-th harmonic of electrodynamic force, i.e., oscillating (AC) voltage

MEMS: imperfect microbeam

The **arched profile**:

from **imperfections** due to microfabrication (*geometrical defects*, *residual stresses*, etc.)

deliberately microfabricated to **exploit bistability** features of curved beams (MEMS *switches and microrelays*)

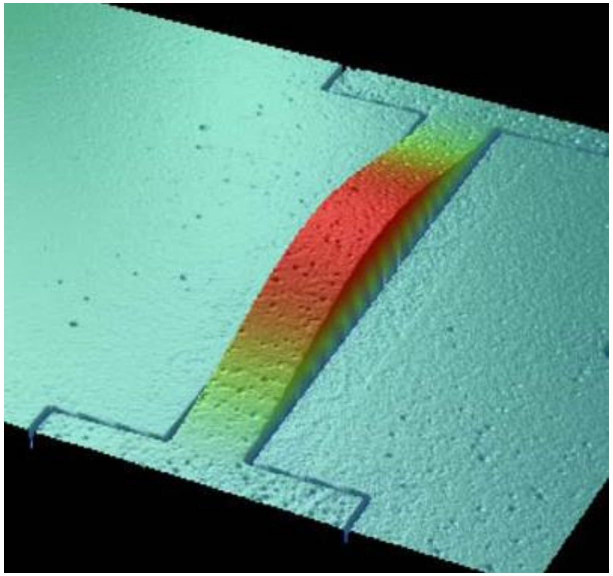

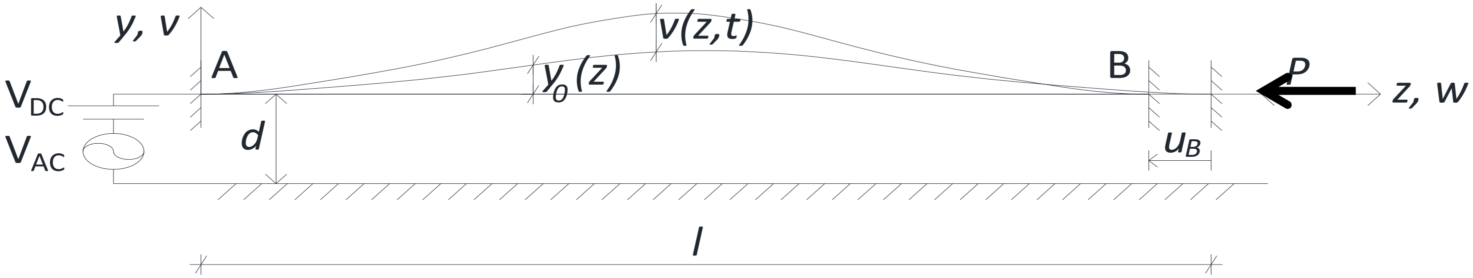

PDE motion

$$\ddot{v} + \xi\,\dot{v} + v^{IV} + \alpha\,(v'' + y_0'') = F_e$$

Geometrical NL $\quad \alpha = n - ka\int_0^1 \left(\frac{1}{2}(v')^2 + v'\,y_0'\right)dz$

Electrostatic+ electrodynamic actuation $\quad F_e = -\gamma\,\dfrac{(V_{DC} + V_{AC}\cos(\Omega\,t))^2}{(d + v(z,t) + y_0(z))^2}$

Imperfect microbeam: reduced order modeling (1)

Single-mode ROMs, with different approximate modeling of potential well

- ***double asymmetric well*** with escape
  (for *bistable* static configuration)
  via combined Galerkin and Padé approximation

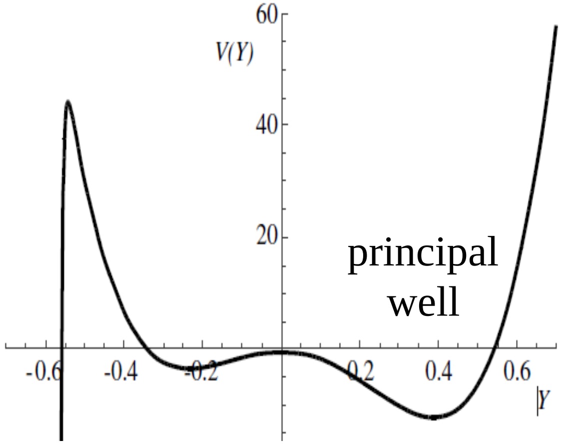

$$\ddot{Y} + 0.17247\dot{Y} - 0.325217 - 256.704Y - 445.54Y^2 + 2866.89Y^3 + (1.2 + V_{AC}\cos(\Omega t))^2 \cdot \frac{0.0168156 + 0.123945Y + 0.353178Y^2 + 0.461589Y^3 + 0.233094Y^4}{1.44(0.596+Y)^6} = 0,$$

(Ruzziconi et al, 2013a)

- ***single well*** with escape
  (for *monostable* static configuration)
  via combined Ritz and Padé

  final model from experimental-based parameter identification also accounting for dynamic integrity concepts

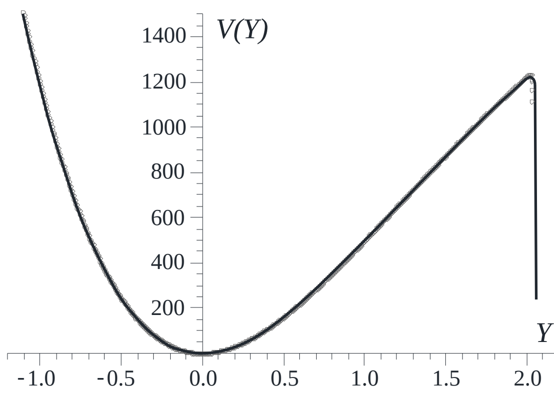

$$\ddot{Y} + 0.085\dot{Y} + 1564.41Y - 1033.40Y^2 + 209.72Y^3 - \frac{1.33949}{(2.05926-Y)^2}(0.7 + V_{AC}\cos(\Omega t))^2 = 0$$

Imperfect microbeam: reduced order modeling (2)

Two-mode Galerkin ROM, to simulate also 1/3 second symmetric superharmonic

$$\begin{cases} \ddot{Y}_1 + 0.085\dot{Y}_1 + 1578.95Y_1 - 1041.09Y_1^2 + 211.50Y_1^3 - 960.38Y_1Y_2 + 37.34Y_1^2Y_2 - 3226.67Y_2^2 \\ + 1936.50Y_1Y_2^2 + 113.87Y_2^3 + 1.85135 \cdot \Psi 1 \cdot (0.7 + V_{AC}\cos(\Omega t))^2 = 0 \\ \ddot{Y}_2 + 0.085\dot{Y}_2 + 1436680Y_2 - 1205870Y_2^2 + 1770350Y_2^3 - 6453.35Y_1Y_2 + 1936.50Y_1^2Y_2 \\ - 480.19Y_1^2 + 341.60Y_1Y_2^2 + 12.45Y_1^3 + 1.85135 \cdot \Psi 2 \cdot (0.7 + V_{AC}\cos(\Omega t))^2 = 0 \end{cases}$$

with numerical evaluation of electric potential integrals

$$\Psi 1 = \int_0^1 \phi_1(z)\Gamma(z)dz, \quad \Psi 2 = \int_0^1 \phi_2(z)\Gamma(z)dz$$

$$\Gamma(z) = \frac{1}{\left(d + v_s(z) + y_0(z) + Y_1\phi_1(z) + Y_2\phi_2(z)\right)^2}$$

- setting Y_2 =0, it reduces to the a single-mode Galerkin model
- due to orthogonality of shape functions ϕ_1 and ϕ_2 (first and second symmetric mode shape) the two equations are decoupled in linear terms

(Ruzziconi et al, 2013b)

NEMS: imperfect carbon nanotube (1)

(*Ruzziconi et al, 2013c ND)*

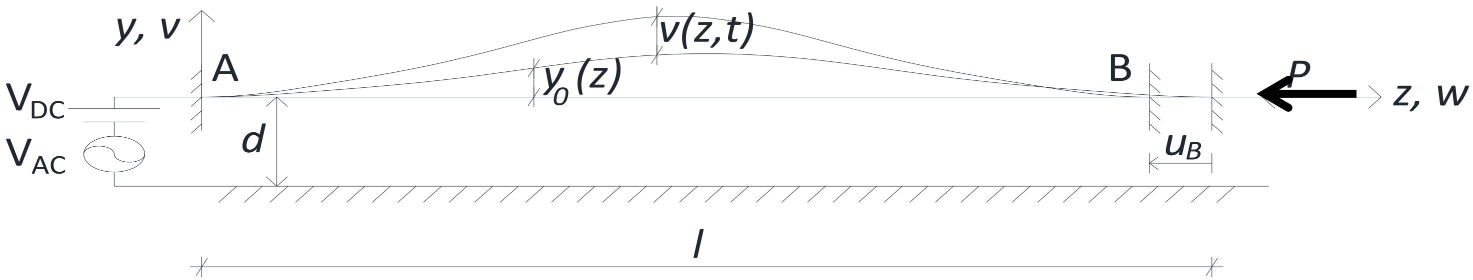

PDE motion $$\ddot{v} + \xi\,\dot{v} + v^{IV} + \alpha\,(v'' + y_0'') = F_e$$

Geometrical NL $$\alpha = n - ka\int_0^1 \left(\tfrac{1}{2}(v')^2 + v'\,y_0'\right)dz$$

Electric force term $$F_e = \frac{(V_{DC} + V_{AC}\cos(\Omega t))^2}{\sqrt{(1 - v - y_0)(1 - v - y_0 + 2R)}(\cosh^{-1}(1 + \frac{1 - v - y_0}{R}))^2}$$

Single-mode ROM

single well with escape

(Galerkin and Padé approximation)

$$\ddot{Y} + 0.01\dot{Y} + 1390.2Y - 11570.8Y^2 + 36392Y^3 - \frac{0.26577}{(0.56866 - Y)^2}\left(V_{DC} + V_{AC}\cos(\Omega t)\right)^2 = 0$$

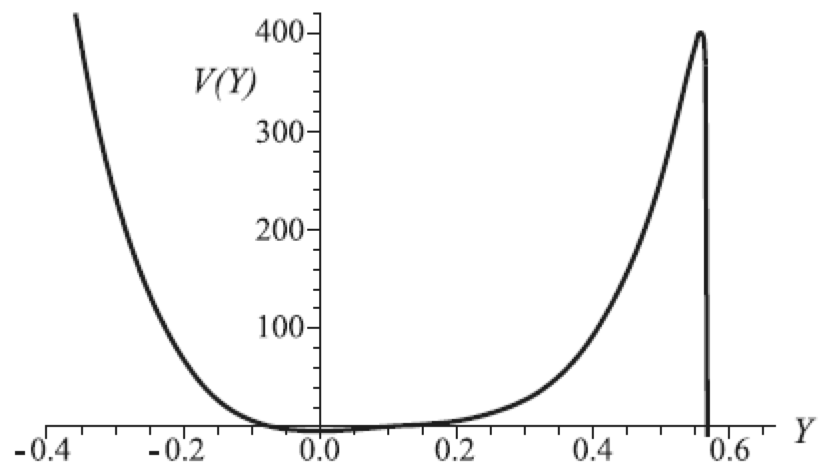

NEMS: imperfect carbon nanotube (2)

(Xu et al, 2016 AM)

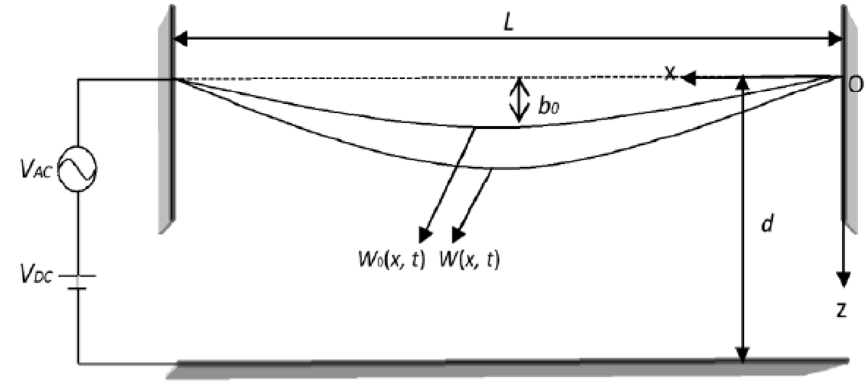

PDE motion

with electric force term

$$\frac{\partial^4 w}{\partial x^4} + \frac{\partial^2 w}{\partial t^2} + c\frac{\partial w}{\partial t} = \alpha_2 F_e + \alpha_1 \left[\int_0^1 \left\{\left(\frac{\partial w}{\partial x}\right)^2 - 2\left(\frac{\partial w}{\partial x}\frac{dw_0}{dx}\right)\right\} dx\right]\left[\frac{\partial^2 w}{\partial x^2} - \frac{d^2 w_0}{dx^2}\right]$$

$$F_e = \frac{(V_{DC} + V_{AC}\cos(\Omega t))^2}{\sqrt{(1 - w - w_0)(1 - w - w_0 + 2R)\left(cosh^{-1}\left(1 + \frac{1 - w - w_0}{R}\right)\right)^2}}$$

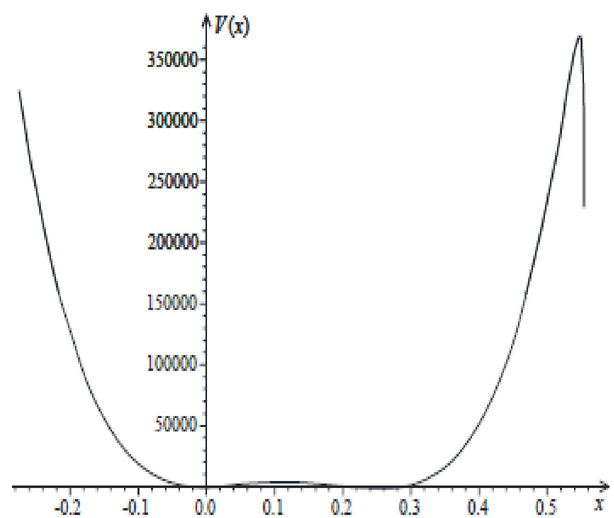

Single-mode ROM

- ***double asymmetric well*** with escape
  (for *bistable* static configuration)
  via combined Galerkin and Padé approximation

$$\ddot{u}_1 + 0.2237\dot{u}_1 + 1.9272 \cdot 10^6 u_1 - 2.2911 \cdot 10^7 u_1^2 + 6.0539 \cdot 10^7 u_1^3$$

$$= (V_{DC} + V_{AC}\cos(\Omega t))^2 \frac{10.7424 - 22.0783u_1 + 2.8898u_1^2 + 20.2295u_1^3}{(0.5574 - u_1)^2}$$

Noncontact atomic force microcantilever

(Hornstein and Gottlieb,2008)

1. **BEAM MODEL** *(Crespo da Silva 1979)*: two coupled PDE (longitudinal and transverse) + BC
2. **INEXTENSIBILITY CONSTRAINT:** single PDE (vertical) + homogeneous BC
3. **MODAL dynamic SYSTEM:** first mode approximation (Galerkin method) → single ODE

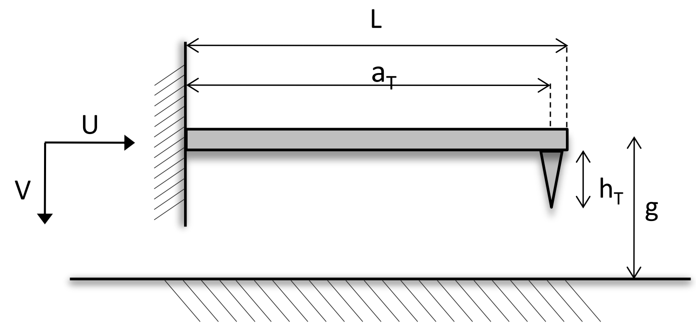

$$\ddot{x}\left(1+\alpha_2 x^2\right)+\alpha_1 x+\alpha_2 x\dot{x}^2+\alpha_3 x^3 =$$

ATOMIC INTERACTION: $$-\Gamma_1\left(1+x+V_g\right)^{-2}$$

DAMPING: $$-\rho_1\dot{x}-\rho_2\dot{x}x^2$$

VERTICAL EXCITATION: $$-\left(\left(\ddot{V}_g+\nu_1\dot{V}_g\right)\right)\nu_2$$

HORIZONTAL EXCITATION: $$+\left(x\mu_1+\mu_2 x^3\right)\left(\ddot{U}_g+\eta_1\dot{U}_g+\eta_2 U_g\right)$$

Hamiltonian system

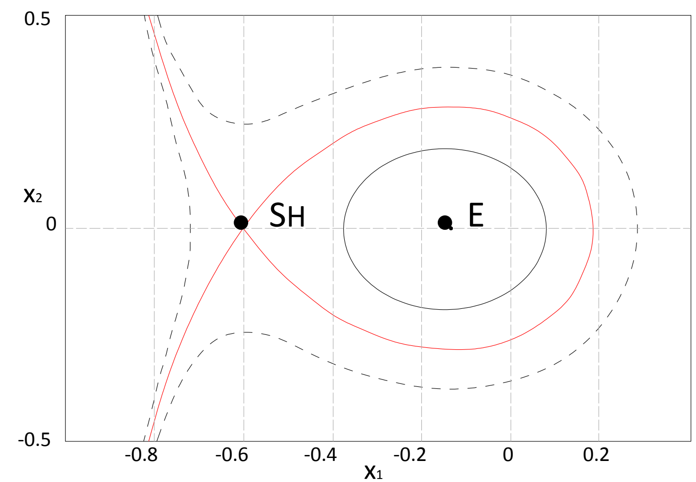

E = Equilibrium solution **SH** = Hilltop Saddle

BOUNDED SOLUTIONS

HOMOCLINIC ORBIT

UNBOUNDED SOLUTIONS

Parametrically excited cylindrical shell (2-dof model)

Modal coupling associated with strong quadratic and cubic nonlinearities and deleterious effects of compressive stresses

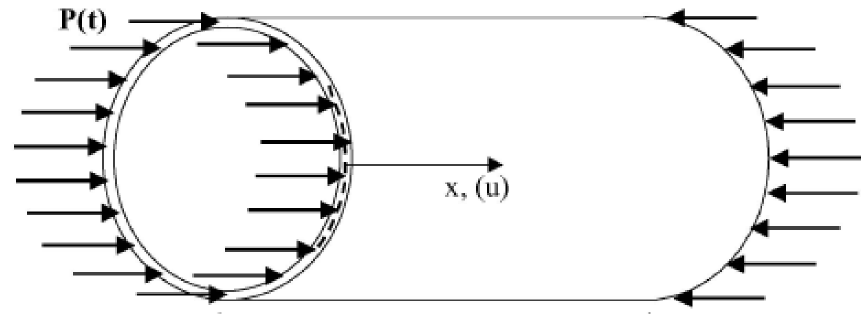

PDE: Donnell nonlinear shallow shell

$$\rho h w_{,tt} + \beta_1 w_{,t} + \beta_2 \nabla^4 w_{,t} + D\nabla^4 w$$
$$= \left(P_0 + P(t) + f_{,yy}\right) w_{,xx}$$
$$+ f_{,xx}\left(w_{,yy} + \frac{1}{R}\right) - 2 f_{,xy} w_{,xy}$$

$$\frac{1}{Eh}\nabla^4 f = -\frac{1}{R} w_{,xx} - w_{,xx} w_{,yy} + w_{,xy}^2$$

P_0 axial static pre-load
$P(t)$ axial harmonic load

Two-mode ROM: linear mode and associated axisymmetric mode with twice the number of waves in axial direction as the linear mode

$$W(\theta,\xi,\tau) = \zeta(\tau)_{11}\cos(n\theta)\sin(m\pi\xi) + \zeta(\tau)_{02}\cos(2m\pi\xi)$$

$$\ddot{\zeta}_{11} + 0.150761\dot{\zeta}_{11} + 1.043914\zeta_{11} + 9.274215\zeta_{11}\zeta_{02} - 1.040775\Gamma_1\cos(\Omega\tau)\zeta_{11}$$
$$-1.043914\Gamma_0\zeta_{11} + 0.274896\zeta_{11}^3 + 0.188199\zeta_{11}\zeta_{02}^2 = 0$$

$$\ddot{\zeta}_{02} + 0.02086\dot{\zeta}_{02} - 4.16310\Gamma_0\zeta_{02} - 4.16310\Gamma_1\cos(\Omega\tau)\zeta_{02} + 69.756712\zeta_{02}$$
$$+ 2.318554\zeta_{02}^2 + 0.094099\zeta_{11}^2\zeta_{02} = 0$$

(Goncalves and Del Prado, 2005)

Parametrically excited cylindrical shell (2-dof model)

Instability of pre-loaded shell resting in a pre-buckling potential well

Unstable post-buckling behavior: when the static load lies between buckling load and the minimum post-critical load a **three well potential** is obtained

Several solutions coexist in the ***pre- and two post-buckling wells*** in addition to large cross-well motions

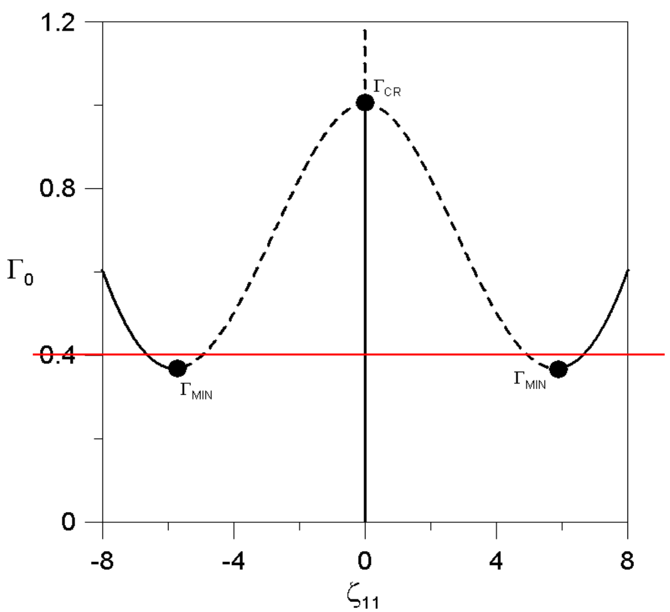

post-buckling response path
(Γ_0 , static load)

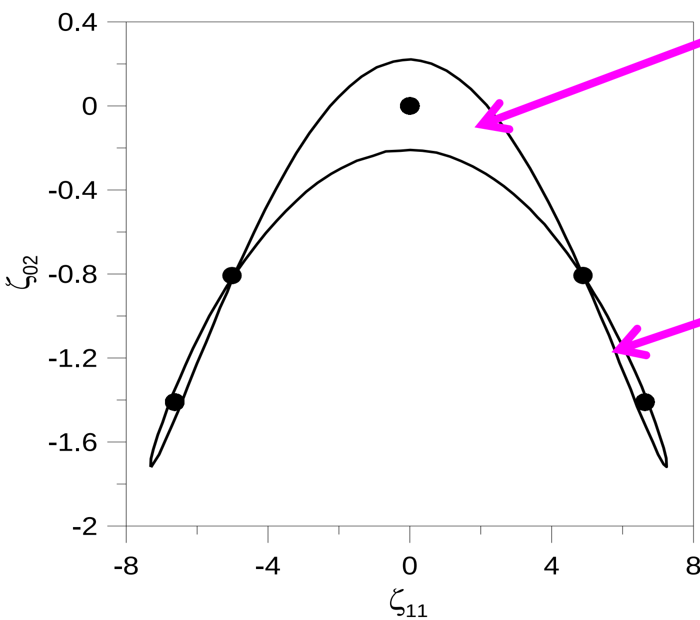

five equilibrium points for Γ_0=0.4
(two heteroclinic and two homoclinic orbits)

γ=0.10; ω=5, δ=0.02, α=0.2, r=0.95; $x_{\text{min/max}}$=±0.28, $y_{\text{min/max}}$=±0.32,

IF, "true" safe basin

1/9

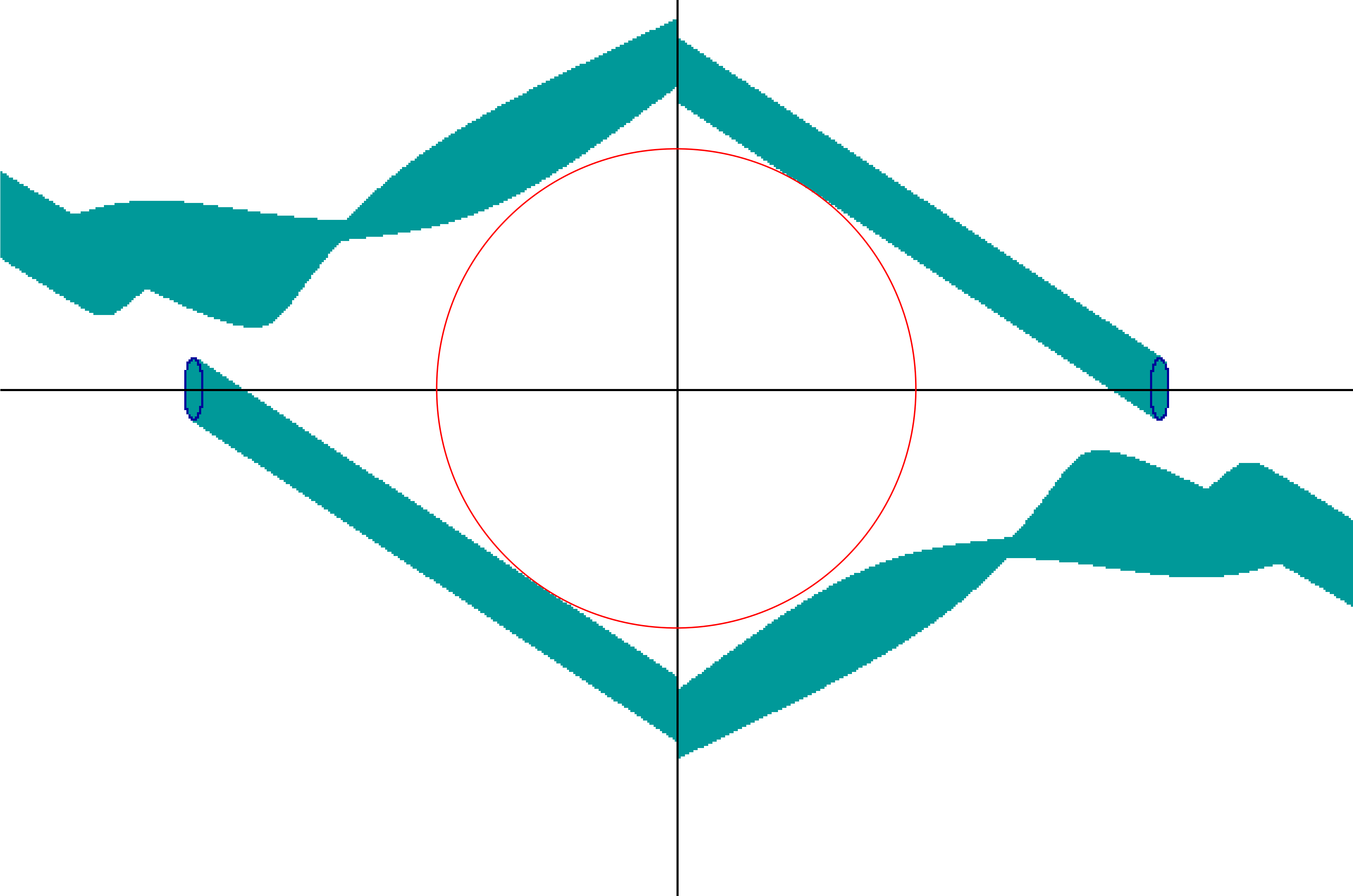

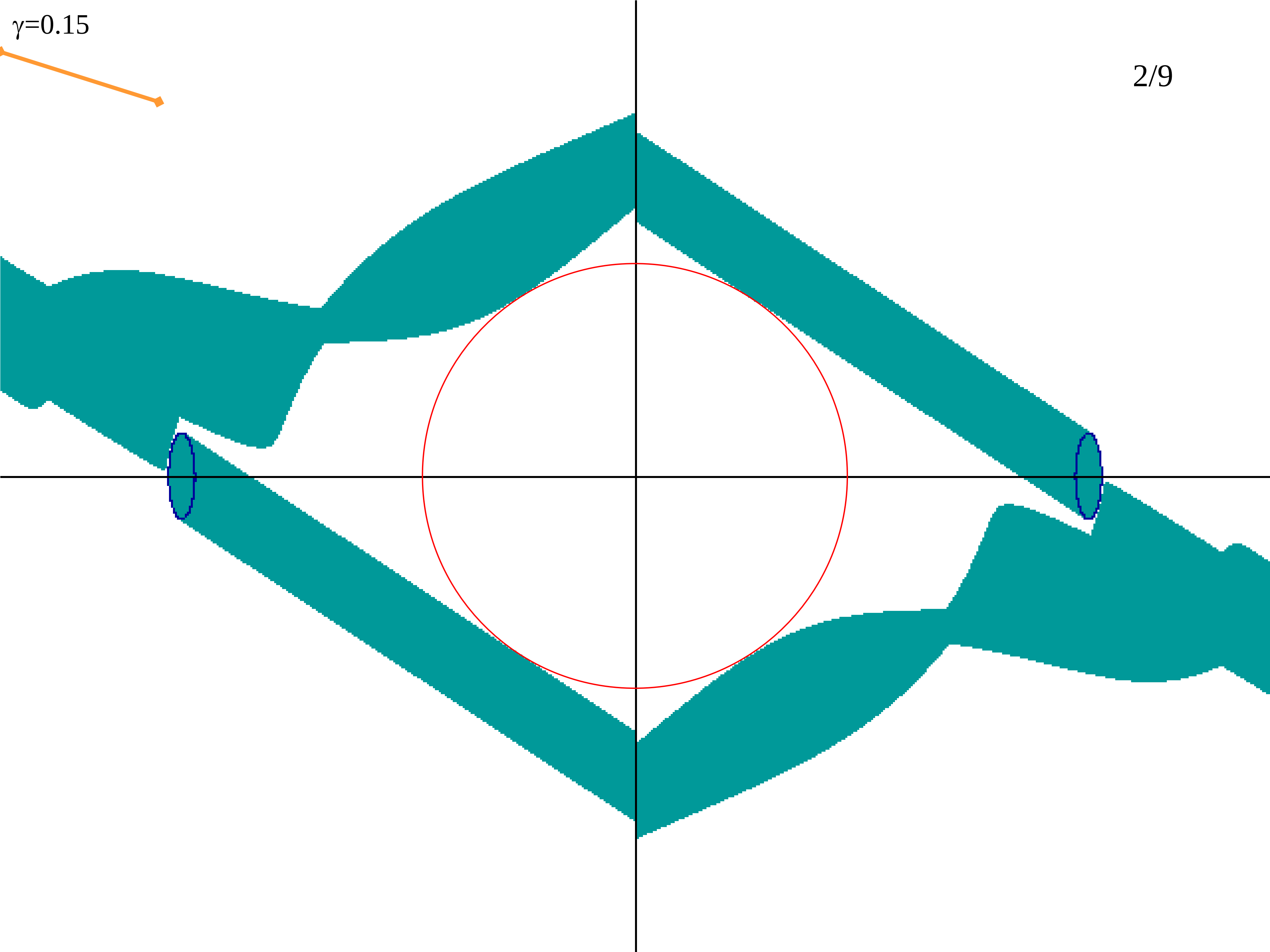

γ=0.15
2/9

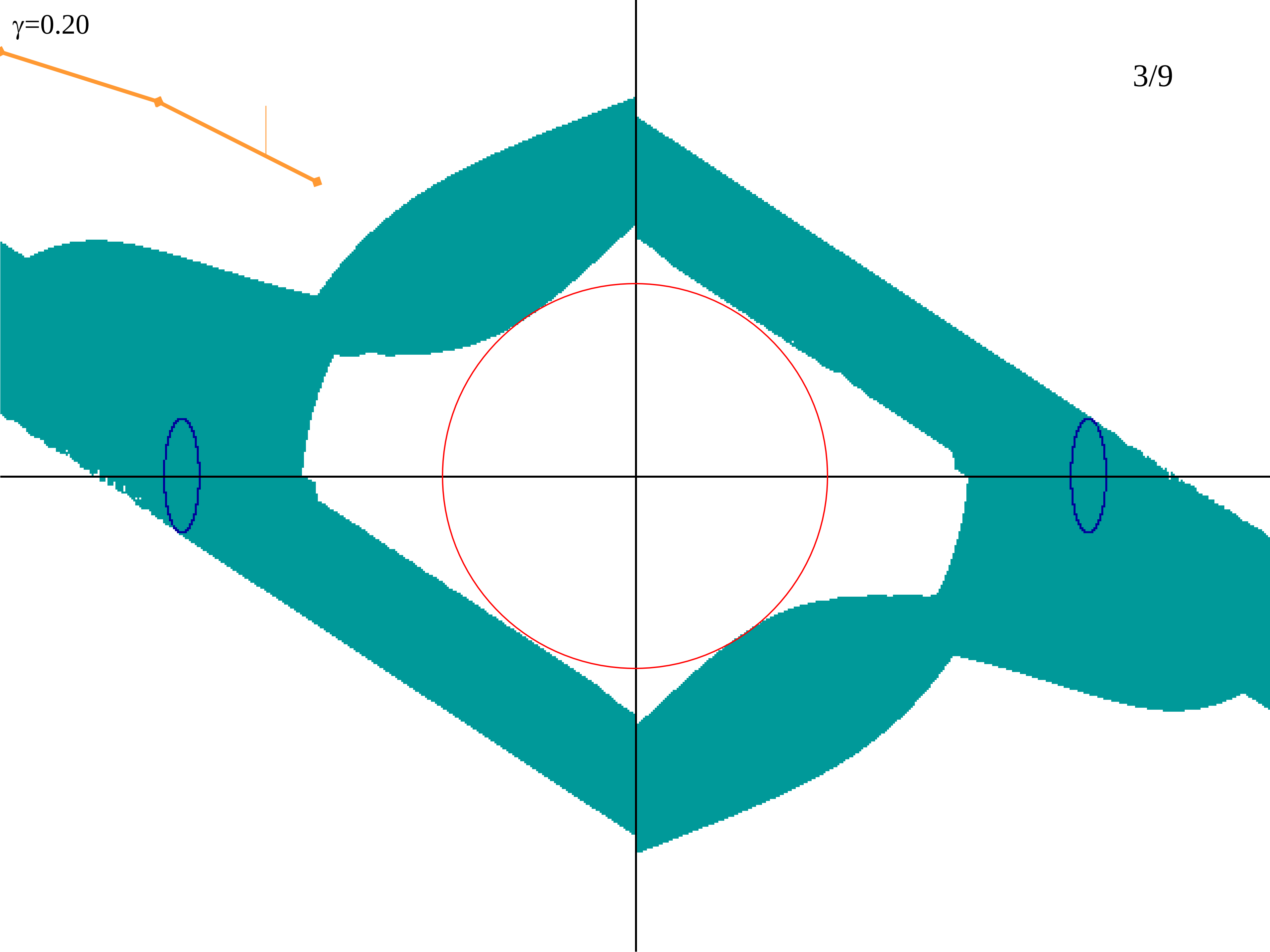

γ=0.20
3/9

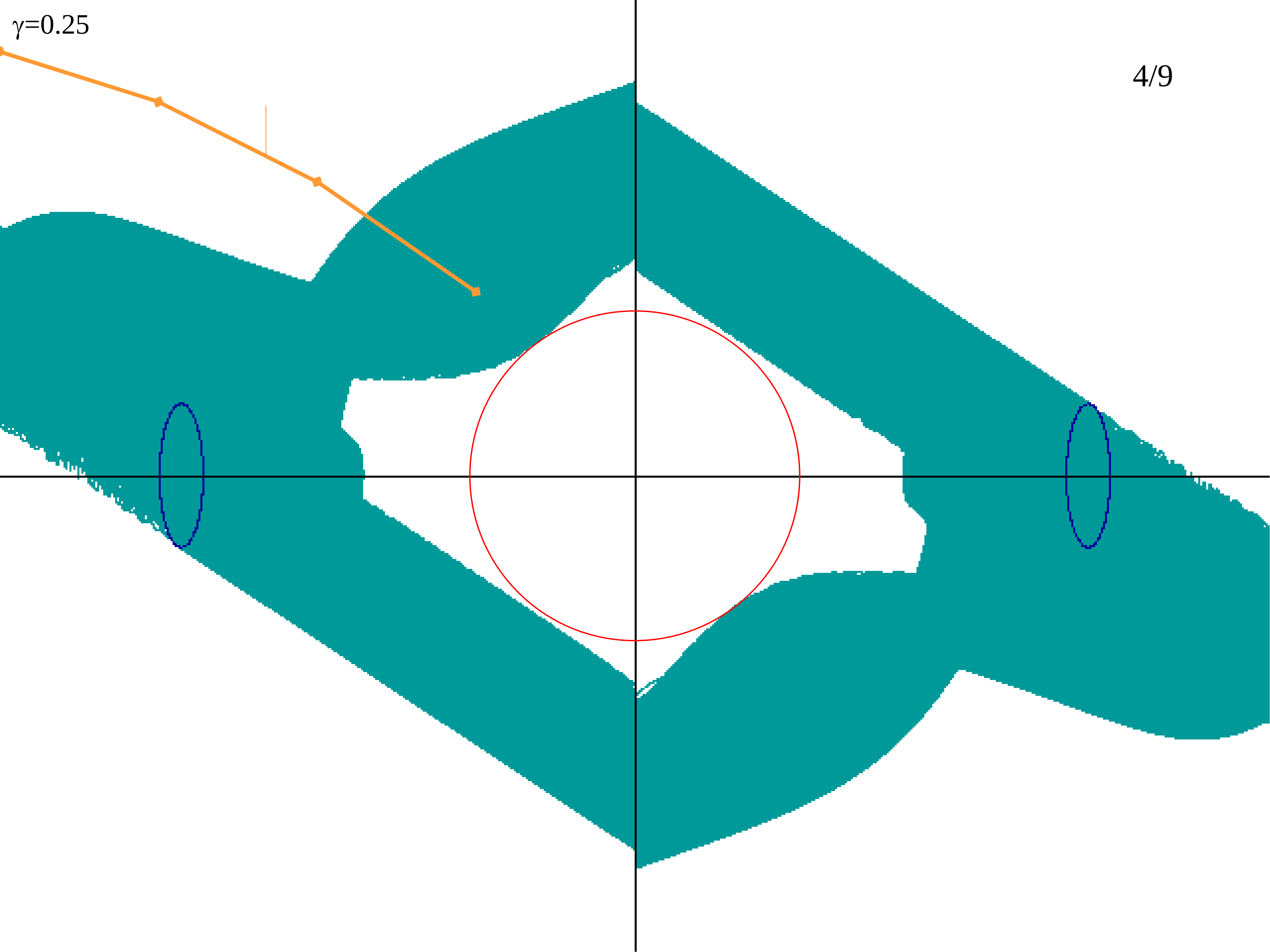
γ=0.25
4/9

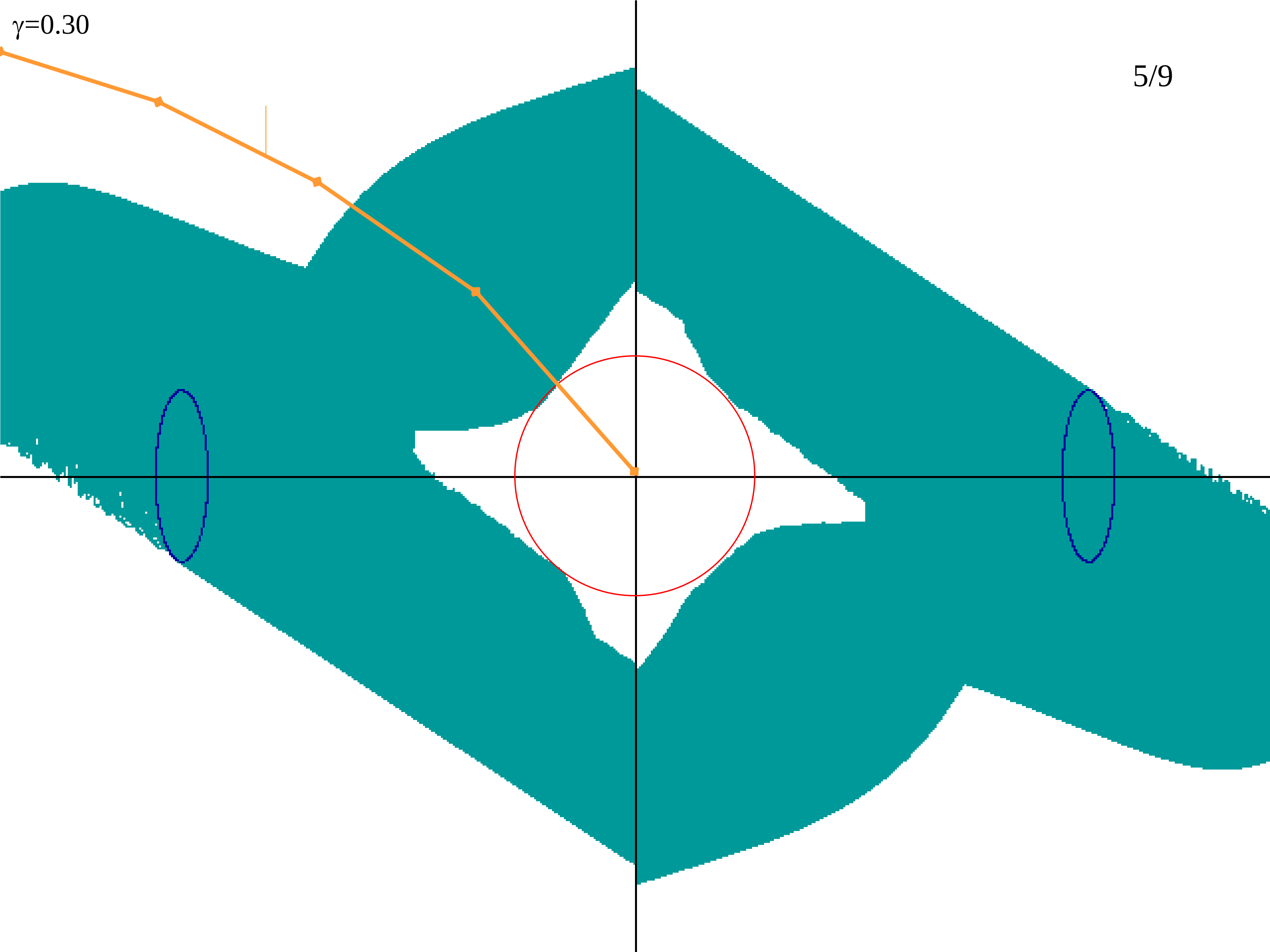

γ=0.30
5/9

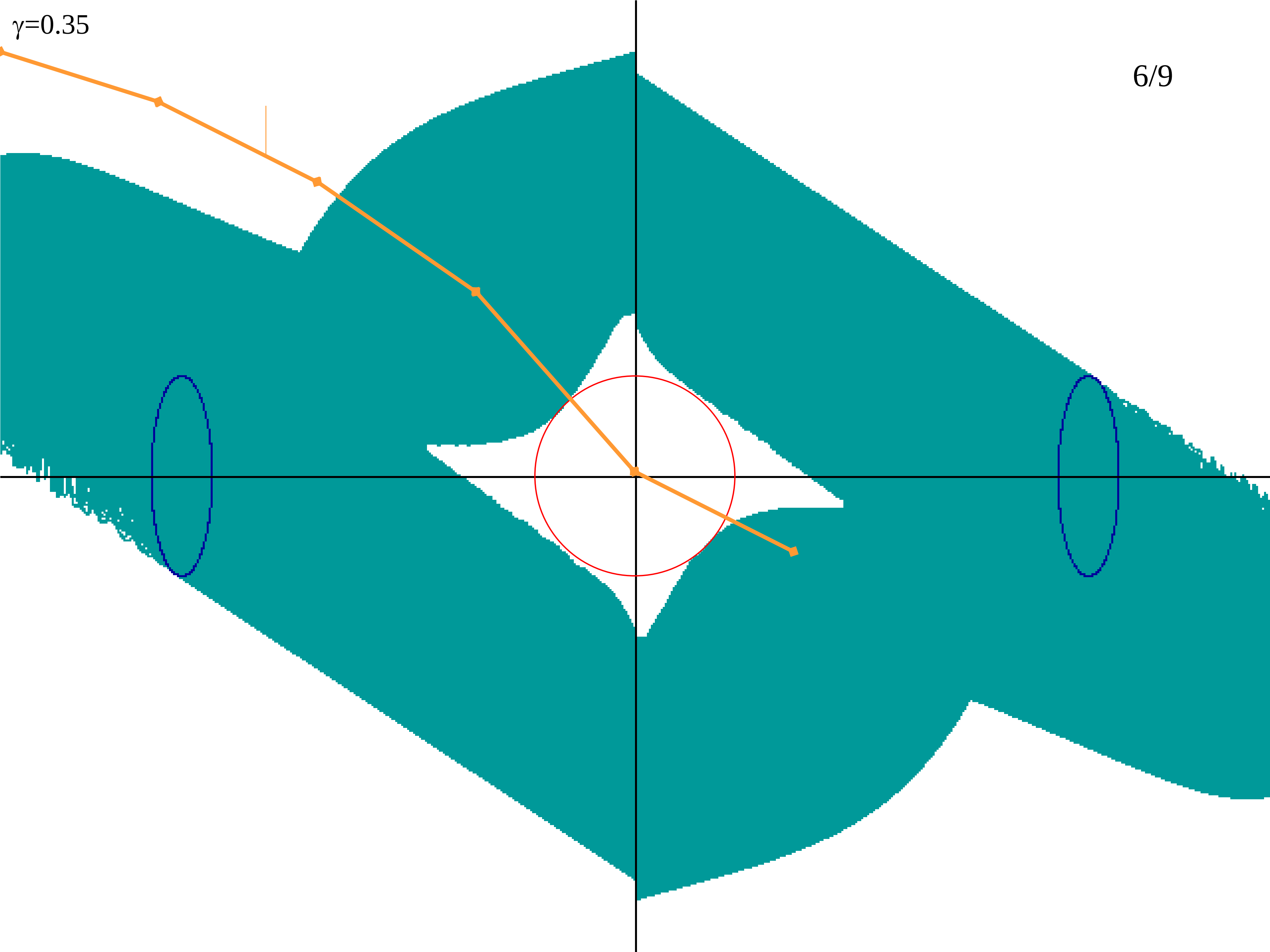

γ=0.35
6/9

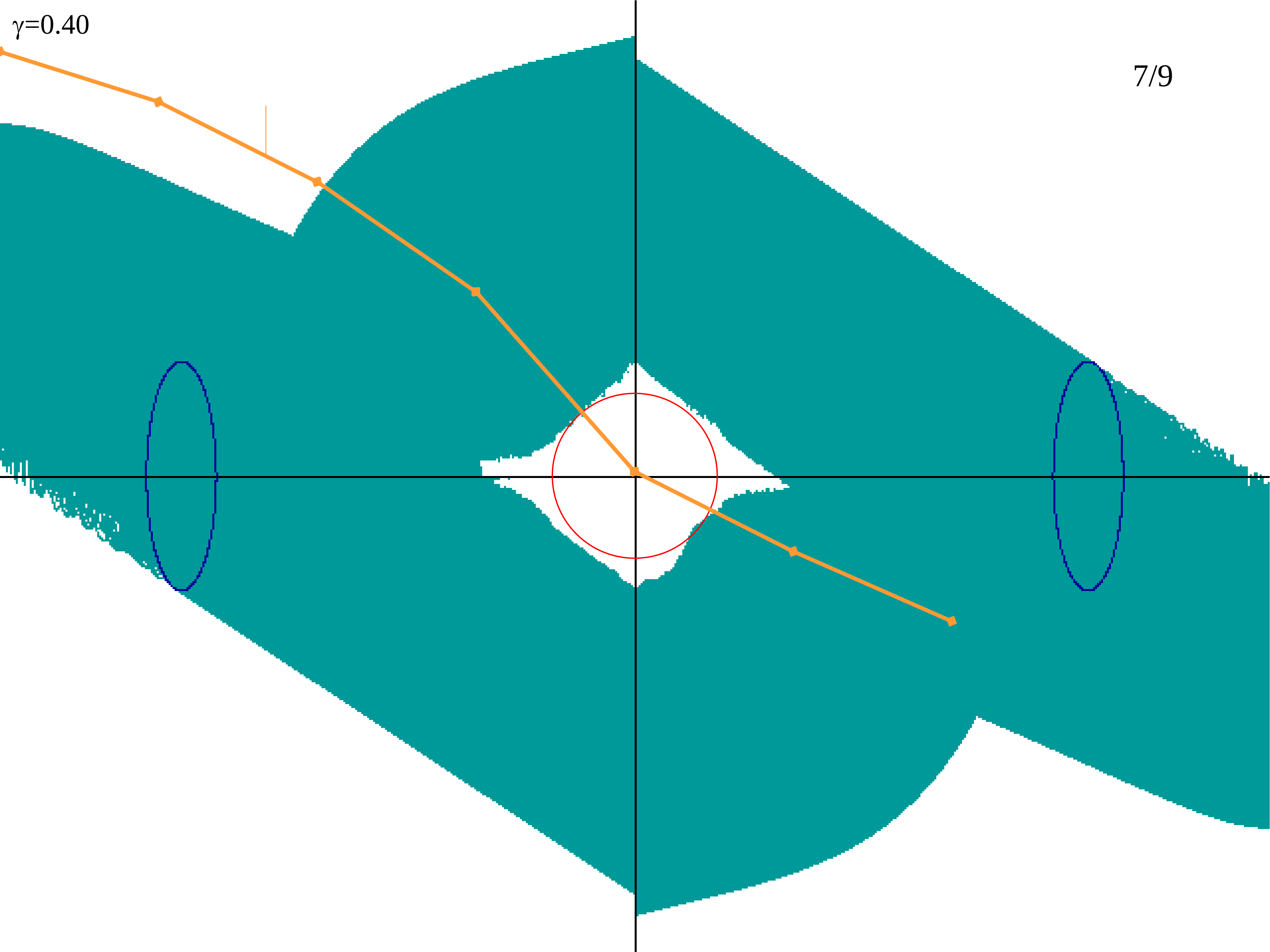
γ=0.40
7/9

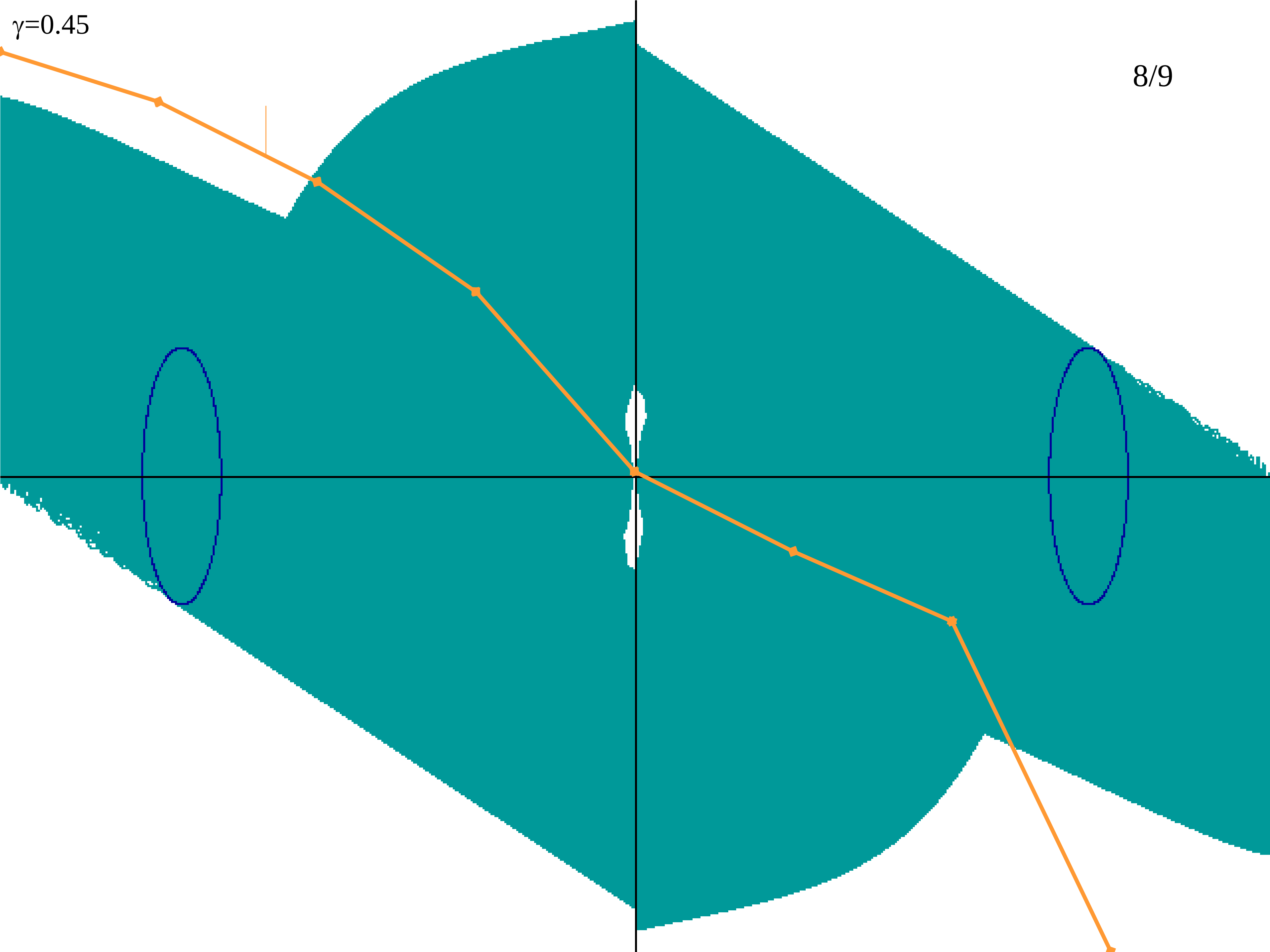

γ=0.45
8/9

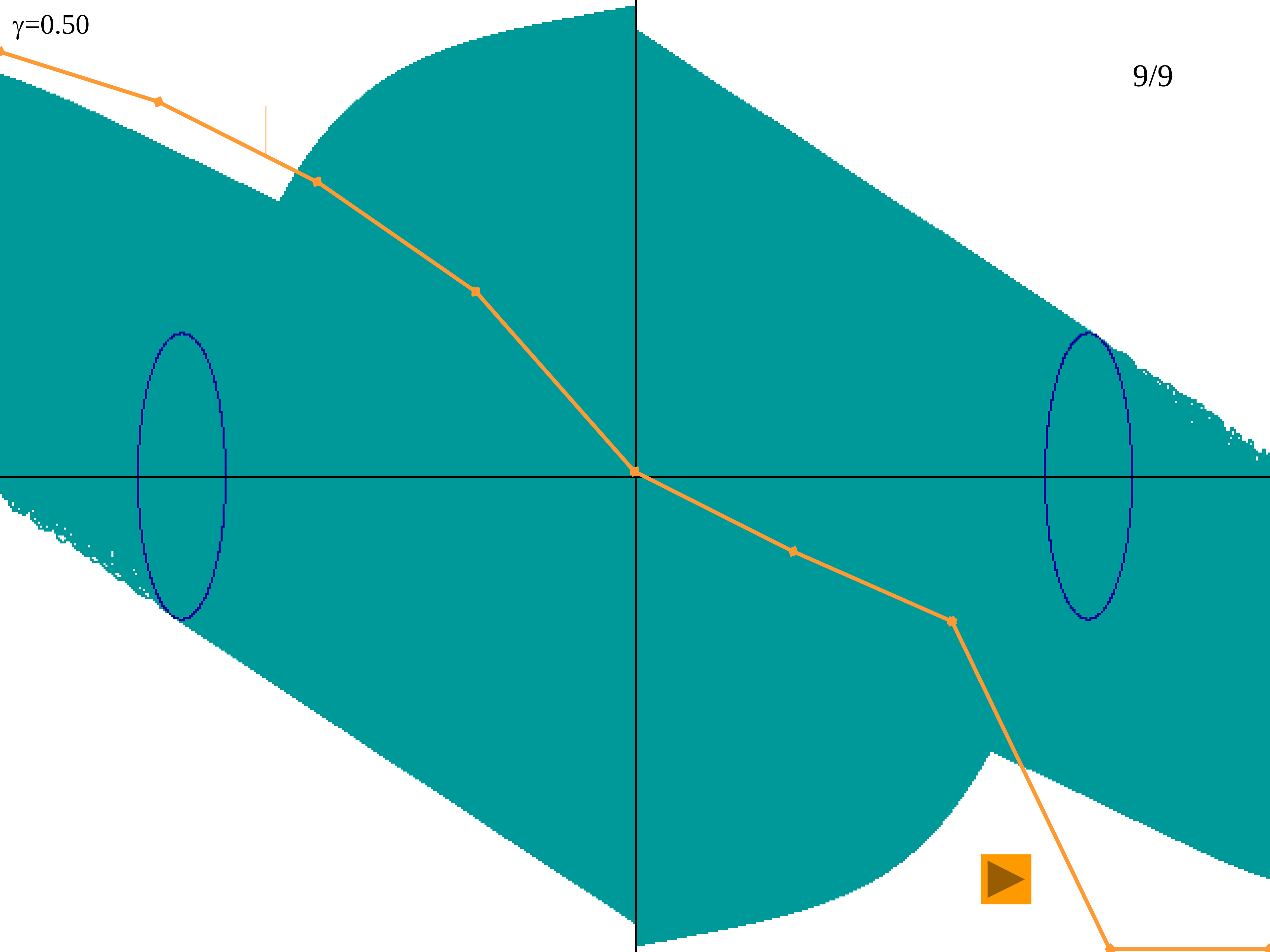

γ=0.50
9/9